# Coronal heating by MHD waves

**Tom Van Doorsselaere · Abhishek K.
Srivastava · Patrick Antolin · Norbert
Magyar · Soheil Vasheghani Farahani · Hui
Tian · Dmitrii Kolotkov · Leon Ofman ·
Mingzhe Guo · Iñigo Arregui · Ineke De
Moortel · David Pascoe**

Tom Van Doorsselaere
Centre for mathematical Plasma Astrophysics, Department of Mathematics, KU Leuven, Ce-
lestijnenlaan 200B bus 2400, B-3001 Leuven, Belgium
E-mail: tom.vandoorsselaere@kuleuven.be

Abhishek K. Srivastava
Department of Physics, Indian Institute of Technology (BHU), Varanasi-221005, India

Patrick Antolin
Department of Mathematics, Physics and Electrical Engineering, Northumbria University,
Newcastle Upon Tyne, NE1 8ST, United Kingdom

Norbert Magyar
Centre for Fusion, Space and Astrophysics, Physics Department, University of Warwick, Coven-
try CV4 7AL, UK

Soheil Vasheghani Farahani
Department of Physics,Tafresh University, Tafresh 39518 79611, Iran

Hui Tian
School of Earth and Space Sciences, Peking University, Beijing 100871, China
Key Laboratory of Solar Activity, National Astronomical Observatories, Chinese Academy of
Sciences, Beijing 100012, China

Dmitrii Kolotkov
Centre for Fusion, Space and Astrophysics, Physics Department, University of Warwick, Coven-
try CV4 7AL, UK
Institute of Solar-Terrestrial Physics SB RAS, Irkutsk 664033, Russia

Leon Ofman
Department of Physics, Catholic University of America, Washington, DC, USA
NASA Goddard Space Flight Center, Greenbelt, MD, USA

Mingzhe Guo
Institute of Space Sciences, Shandong University, Weihai 264209, People's Republic of China
Centre for mathematical Plasma Astrophysics, Department of Mathematics, KU Leuven, Ce-
lestijnenlaan 200B bus 2400, B-3001 Leuven, Belgium

Iñigo Arregui
Instituto de Astrofísica de Canarias, 38205, La Laguna, Tenerife, Spain
Departamento de Astrofísica, Universidad de La Laguna, 38206, La Laguna, Tenerife, Spain

Ineke De Moortel
School of Mathematics and Statistics, University of St Andrews, North Haugh, St Andrews,
KY16 9SS, UK

**Abstract** The heating of the solar chromosphere and corona to the observed high temperatures, imply the presence of ongoing heating that balances the strong radiative and thermal conduction losses expected in the solar atmosphere. It has been theorized for decades that the required heating mechanisms of the chromospheric and coronal parts of the active regions, quiet-Sun, and coronal holes are associated with the solar magnetic fields. However, the exact physical process that transport and dissipate the magnetic energy which ultimately leads to the solar plasma heating are not yet fully understood. The current understanding of coronal heating relies on two main mechanism: reconnection and MHD waves that may have various degrees of importance in different coronal regions. In this review we focus on recent advances in our understanding of MHD wave heating mechanisms. First, we focus on giving an overview of observational results, where we show that different wave modes have been discovered in the corona in the last decade, many of which are associated with a significant energy flux, either generated in situ or pumped from the lower solar atmosphere. Afterwards, we summarise the recent findings of numerical modelling of waves, motivated by the observational results. Despite the advances, only 3D MHD models with Alfvén wave heating in an unstructured corona can explain the observed coronal temperatures compatible with the quiet Sun, while 3D MHD wave heating models including cross-field density structuring are not yet able to account for the heating of coronal loops in active regions to their observed temperature.

**Keywords** Sun: corona · Sun: waves

# 1 Introduction

Coronal heating is a long-standing problem. It is quite clear that the energy for the hot corona comes from the convective motions of the solar photosphere, and that the magnetic field plays a key role in it. However, how the energy is transported and dissipated is still not fully understood. Proposed heating mechanisms are classified based on the comparison of the convective time scales and the Alfvén transit time in the corona. Slow driving of the magnetic field that produces reconnection and energy release in current sheets and null points, is referred to as DC heating mechanisms (Parker, 1986). Fast driving of the magnetic field, is known as MHD wave heating (e.g. Alfvén, 1947) and AC heating mechanisms.

DC heating mechanisms consider the slow stressing of the coronal magnetic field. It leads to current sheets where Ohmic dissipation is at work, or to Parker's idea of nanoflares. In the latter idea, the magnetic field is tangled because of the photospheric motions, so that it evolves into a non-potential state. This magnetic energy is then released into the plasma by reconnection, resulting in localised heating and thus nanoflares. DC heating mechanisms have received a lot of attention over the years in numerical modelling and observations (e.g. Gudiksen and Nord-

Rosseland Centre for Solar Physics, University of Oslo, PO Box 1029 Blindern, NO-0315 Oslo, Norway

David Pascoe
Centre for mathematical Plasma Astrophysics, Department of Mathematics, KU Leuven, Celestijnenlaan 200B bus 2400, B-3001 Leuven, Belgium

lund, 2005; Reep et al., 2013; Rempel, 2017; Warnecke et al., 2017; Srivastava et al., 2019).

In this review, we focus on AC heating mechanisms. In these heating mechanisms, the convective motions launch disturbances that travel into the corona, usually in the form of magnetohydrodynamic (MHD) waves. In the corona, the wave energy has to be dissipated to heat the plasma. This is non-trivial, because many wave modes damp only on resistive time scales in a homogeneous plasma, and damping times are proportional to the magnetic Reynolds number. In the solar corona, the Reynolds number is very large, on the order of $10^{14}$, which would produce unrealistically long heating times, compared to the coronal cooling timescale. Cross-field inhomogeneity enables physical processes that produce a cascade of wave energy to small spatial scales where dissipative processes may act and heat the plasma more rapidly. In recent years, there has been a drive towards (1) observational characterisation of wave energy content in the corona, and (2) numerical modelling of wave heating, focusing on the energy input, the energy propagation and the energy dissipation. Here, we aim to give an overview of these recent results.

For material beyond the current review, we refer the reader to, for example, Aschwanden (2019).

1.1 Brief historical overview

The idea for heating the solar corona by MHD waves has been around for more than half a century. An overview of the early ideas before the 80s can be found in Kuperus et al. (1981). In those years, it was realised that it is necessary to generate small scales in order to damp the wave energy in a timely manner. Heyvaerts and Priest (1983) developed the theory of phase mixing, while resonant absorption (Chen and Hasegawa, 1974) was applied to the corona for the first time by Ionson (1978). Subsequently, the MHD wave energy input and transmission into coronal loops was studied in key papers such as Hollweg (1984). Later on, the efficiency of the heating by resonant absorption was calculated in 1D numerical models of loops (Poedts et al., 1990, among others), and in 3D models (Ofman et al., 1994, and follow-up works), even resulting in forward modelled coronal loops (Belien et al., 1996), motivated by early high resolution soft X-ray observations of coronal loops that became available from the Yohkoh satellite.

In hindsight, it is amazing that these early papers worked so well and were so relevant, given that no direct observational evidence was available back then on the presence of MHD waves in the solar corona. Indeed, although substantial, only indirect evidence existed of the potentially important role of MHD waves in the solar atmosphere. Such evidence was based on the strong emission and broad non-thermal line widths in the upper chromosphere, transition region and corona with observations from Skylab (Feldman et al., 1988) and HRTS (High-Resolution Telescope and Spectrograph, Dere and Mason, 1993). This changed dramatically with the launch of SOHO (Solar and Heliospheric Observatory) and TRACE (Transition Region And Coronal Explorer). Data from the former were used to show the presence of slow waves in the corona (Chae et al., 1998; Ofman et al., 1999; Berghmans and Clette, 1999), while data from the latter revealed the presence of transverse, post-flare loop oscillations (Nakariakov et al., 1999; Schrijver et al.,

1999; Aschwanden et al., 1999). An overview of the contextualisation of earlier models with those observational findings is given in Walsh and Ireland (2003); Ofman (2005).

LCR models (named after the usual symbols in electric components for inductance L, capacitance C and resistance R) were also developed extensively for MHD waves in coronal loops (see Stepanov et al., 2012, and reference therein). In such models, the magnetic twist in the loop behaves as a current system with its source in the photosphere and equivalent electric resistivity and inductance in the corona (see e.g., Spicer, 1977; Carlqvist, 1979). However, it is still unclear how this LCR model relates to MHD models of coronal loop oscillations (based on e.g. Edwin and Roberts, 1983). Moreover, since no development of these models was made in the last years, we will omit them from this review.

1.2 Observational motivation

Starting with the advent of high resolution space-based observations of the solar corona in soft X-ray and EUV in the 90s, there is now an avalanche of new MHD wave modes detected in the solar corona, as described in detail by De Moortel and Nakariakov (2012). Their consequences for heating the corona are discussed in Arregui (2015).

Another major paradigm change in our perception of MHD waves in the solar atmosphere came from ground-based observations with *CoMP* (Tomczyk et al., 2007), which showed the omnipresence of these waves in the solar corona, and spectroscopic and imaging from space with *Hinode*, which, thanks to its high resolution, allowed to better quantify the amount of energy available for the corona (De Pontieu et al., 2007). Moreover, *SDO/AIA* revealed the existence of many new wave modes and made more detailed observations of previously observed coronal waves (for a review, see Liu and Ofman, 2014).

The improvement in spatial, spectral and temporal resolution of instrumentation also meant that MHD waves could be characterised in terms of their slow, fast or Alfvén nature, as well as their wave numbers (see the review by De Moortel and Nakariakov, 2012). Indeed, high spatial resolution and high sensitivity allows to distinguish transverse motions of the waveguides as well as the compressibility of the gas from density diagnostics, while high spectral and temporal resolution allows to relate these quantities to the evolution of the Doppler and non-thermal velocities, thereby determining the 3D motion of the plasma produced by the waves (see e.g. Fujimura and Tsuneta, 2009; Kitagawa et al., 2010; Wang, 2016; Hinode Review Team et al., 2019, chapter 6.1).

Lastly, multi-wavelength observations with instruments such as those of *Hinode* and *IRIS*, or through coordinated observations with space and ground-based observatories allowed to simultaneously scan several layers of the solar atmosphere. Although a complicated task, this provides the propagation history of the wave, which is essential to determine wave processes such as reflection and refraction, and in particular mode conversion and dissipation of MHD waves for coronal heating (Arregui, 2015).

**Table 1** Overview of detected wave energy fluxes. The first column shows the structure in the solar atmosphere with the observed wave mode (second column) and the observing instrument (third column). The fourth column shows the estimated energy flux, as found by the reference mentioned in the fifth column. If a cell is left empty, the value from the previous line are meant.

| Structure | Wave mode | Instrument | Energy flux (W m$^{-2}$) | Reference |
|---|---|---|---|---|
| coronal arcade | propagating kink | CoMP | 100 | Tomczyk et al. (2007) |
| coronal funnels | quasi-periodic fast wave trains | AIA | $(0.1 - 2.6) \times 10^4$ | Liu et al. (2011) |
| | | simulations | $3.7 \times 10^5$ | Ofman et al. (2011) |
| | | AIA | $1.8 \times 10^2$ | Ofman and Liu (2018) |
| magnetic pores | Alfvén waves | ROSA | $1.5 \times 10^4$ (locally) | Jess et al. (2009) |
| | | | 240 (globally averaged) | |
| | propagating slow sausage | DST | $3.5 \times 10^4$ | Grant et al. (2015) |
| fibrils | propagating kink | ROSA | $4.3 \times 10^3$ | Morton et al. (2012) |
| | propagating fast sausage | | $1.17 \times 10^4$ | |
| spicules | Alfvén waves | SST | $10^5$ | Srivastava et al. (2017) |
| | kink | | $10^2 - 10^4$ | this review, based on De Pontieu et al. (2012) |

## 2 Observations

Below, we describe recent detections of wave power in the solar atmosphere. We summarise the energy fluxes in Table 1 to give a clear overview.

### 2.1 Impulsively excited standing kink waves

Often flares and low coronal eruptions (LCEs) are seen to excite standing kink waves in coronal loops (Zimovets and Nakariakov, 2015). Goddard et al. (2016a) and Nechaeva et al. (2019) performed a statistical study of these types of events and found that the loops oscillate with an amplitude between 1-10 Mm and periods between 1-28 min. While the coronal impulsive event that causes the oscillations is apparent, the exact mechanism for their excitation is not well understood. Several possibilities were investigated in the literature: internal and external (gas or magnetic) pressure drivers (Terradas et al., 2007; McLaughlin and Ofman, 2008; Pascoe et al., 2009; Selwa and Ofman, 2009; Pascoe and De Moortel, 2014), loop contraction (Russell et al., 2015; Pascoe et al., 2017), or collision of flows (Antolin et al., 2018a; Pagano et al., 2019, even though these would result in propagating waves). More information about observations of impulsively excited standing waves can be found in the review by Nakariakov et al. (2021).

The energy available in impulsively excited standing waves and the fraction that is dissipated remains to be characterised from observations. An energy analysis based on bulk plane Alfvén waves is too simplistic because kink mode energy is localised in space (Goossens et al., 2013). Magnetic and plasma structures act as frequency filters, trapping part of the available energy and distributing it along and across the coronal field. Wave energy propagation, once filtered by the structure is localised in space. Energy flows into the resonance because of the jump in the radial component of the Poynting vector (Arregui et al., 2011), as shown in Fig. 1. Then, it propagates and dissipates along the field in a way determined by the density profile and dissipative coefficients.
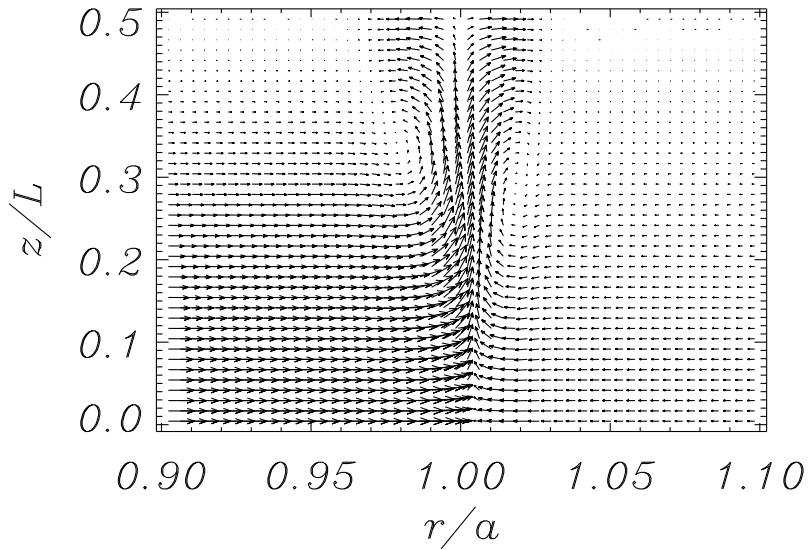
**Fig. 1** Spatial distribution of the Poynting vector in the $(r, z)$-plane around the resonant position at $r/a = 1$ for a standing kink mode in a loop with a density contrast of 10 and a non-uniform layer of length $l/a = 0.2$. The magnetic Reynolds number is $R_{\mathrm{m}} = 10^6$. Figure modified from Arregui et al. (2011).

Terradas and Arregui (2018) considered each part of the sequence of physical processes that would enable to heat a typical coronal waveguide from the energy contained in a typical transverse oscillation. Each part of the sequence has its characteristic time and spatial scales. The damping time is determined by the cross-field plasma and field structuring. The energy cascade to small scales is determined by a phase mixing length that also depends on the cross-field variation of the Alfvén speed. The onset of resistive dissipation and its duration depend on the Reynolds number and the cross-field plasma variation. Considering typical values of these quantities we cannot expect resistive diffusion to operate during the oscillation process. Any observational evidence about wave heating by resistive damping of impulsively excited standing waves will come from the observation of indirect consequences. According to (Terradas and Arregui, 2018), for a loop displacement of the order of the radius and typical loop parameters, all the kinetic and magnetic energy of a typically observed single kink mode is of the order of $10^{19}$ J. Simple energy conservation calculations indicate that, even if we were able to concentrate in a typical resonant layer and transform into internal energy all the kinetic and magnetic energy of a typically observed single kink mode, we could just obtain a temperature increase of about $10^5$ K (Terradas and Arregui, 2018).

When an ensemble of mini-tubes are considered, filling factors can be employed (Van Doorsselaere et al., 2014), which leads to an energy flux reduction directly related to the filling factor. Although resonant damping and mode coupling are robust in coronal loop models with rather arbitrary continuous plasma distributions,

the multi-strand structure of loops could be quickly destroyed due to instabilities in individual strands and their interaction (Magyar and Van Doorsselaere, 2016).

## 2.2 CoMP waves

Prevalent propagating waves were reported (Tomczyk et al., 2007; McIntosh et al., 2011) from observations of both the Coronal Multi-channel Polarimeter (CoMP, Tomczyk et al., 2008) and the Atmospheric Imaging Assembly (AIA, Lemen et al., 2012) on board the Solar Dynamics Observatory (SDO). Using CoMP observations, Tomczyk et al. (2007) found ubiquitous upward propagating disturbances along off-limb coronal loops in the Doppler shift of the Fe XIII 10747 Å line (Figure 2). Since the Doppler shift refers to the motion along the line of sight (LOS) and the magnetic field lines in the off-limb corona are largely perpendicular to the LOS, these disturbances are essentially signatures of transverse MHD waves. The propagation speed was found to be from a few hundred km s$^{-1}$ to 2000 km s$^{-1}$, which is on the order of the coronal Alfvén speed. Based on these characteristics, Tomczyk et al. (2007) and Tomczyk and McIntosh (2009) interpreted these transverse waves as Alfvén waves. They found a power-law spectrum of the Doppler shift with a spectral index of about 1.5, consistent with isotropic MHD turbulence. The power spectrum of the observations shows a peak around 3.2 mHz (period of 5 minutes). The velocity amplitude is only 0.5 km s$^{-1}$, and the energy flux of these waves appears to be at least three orders of magnitude lower than that required to balance the radiative losses of the quiet corona. The low-amplitude is likely due to the low spatial resolution of CoMP ($\sim 9''$) and the line-of-sight integration resulting in spatial averaging of the waves. Similar results were also found in open-field regions (Morton et al., 2015). By carefully analyzing the displacement of coronal structures observed by the much higher-resolution AIA instrument ($\sim 1.5''$), McIntosh et al. (2011) found much larger velocity amplitudes, i.e., $\sim 20$ km s$^{-1}$, for these transverse waves. They estimated the energy flux of the waves as $\sim 100$ W m$^{-2}$ and found that the waves have sufficient energy to power the quiet corona and fast solar wind. However, the observed wave energy flux is still much lower than that required to heat the active region corona ($\sim 2000$ W m$^{-2}$).

   The interpretation of these waves as Alfvén waves was controversial. As argued by Van Doorsselaere et al. (2008), in cylindrical plasma structures these waves appear to be more appropriately interpreted as fast-mode kink waves rather than Alfvén waves. However, others claimed that these waves could be called Alfvénic waves as the major restoring force for these waves is definitely magnetic tension (Goossens et al., 2009; McIntosh et al., 2011), they carry parallel vorticity (Goossens et al., 2012) and they are inherently coupled to the local azimuthal Alfvén waves (Pascoe et al., 2010). This mode is also called surface Alfvén wave or resonantly damped kink mode. At the end, the heating will come from azimuthal Alfvén wave dissipation. The global eigen-mode just plays the role of trapping/chanelling the energy from around/below. A well defined structure is not needed, as shown by Terradas et al. (2008b); Rial et al. (2010); Pascoe et al. (2011).
Despite the debate on the nature and terminology for these waves, the discovery of these propagating transverse waves has caught the attention of many researchers in the field. There are at least two reasons for this. First, they allow us to map
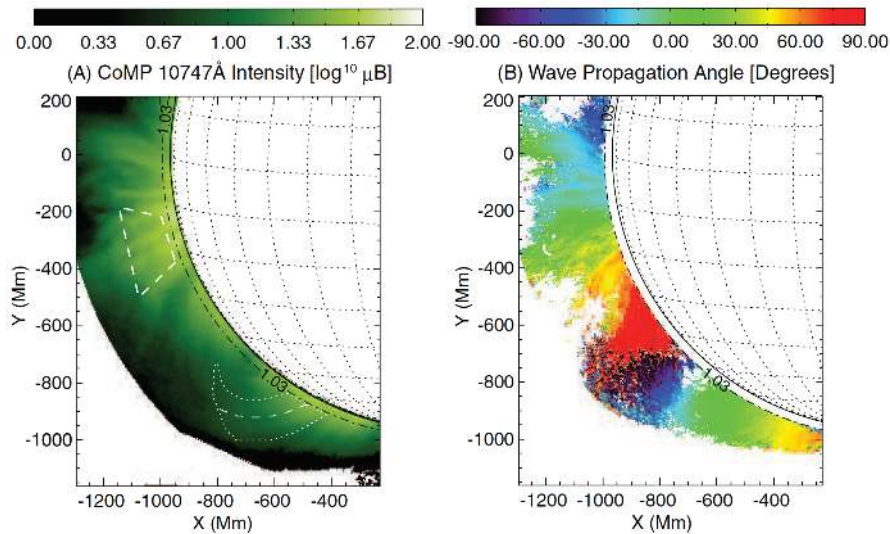
**Fig. 2** Images of the Fe XIII 10747 Å line intensity and the wave propagation angles derived from the Doppler shift of Fe XIII 10747 Å in part of the corona observed by CoMP. Adapted from Tomczyk and McIntosh (2009).

the global coronal magnetic field based on the technique of coronal seismology (Magyar and Van Doorsselaere, 2018; Anfinogentov and Nakariakov, 2019; Yang et al., 2020a,b). Second, their ubiquity means they could potentially play an important role in coronal heating. The observed waves show a discrepancy between the outward and inward wave power (Tomczyk and McIntosh, 2009), a property that resonantly damped wave models seem to capture well (Verth et al., 2010; Pascoe et al., 2010), and that is also observed in-situ in the solar wind (see the review by Bruno and Carbone, 2013). A recent study by Montes-Solís and Arregui (2020) considers a distinct power generated at loop foot-points as an additional source of discrepancy. It shows that, if present, it would affect obtaining quantitative evidence for resonant damping.

The origin of the waves detected by CoMP has recently been linked to the Sun's internal acoustic oscillations, and in particular to p-modes. Indeed, Morton et al. (2019) have shown that there is a distinct excess of wave power at the usual p-mode frequency of $3-5$ mHz, across the solar cycle and different coronal structures (or regions) in the Sun (Morton et al., 2016). The authors further show that the usual Alfvénic fluctuations observed with SDO/AIA (McIntosh et al., 2011) have the same characteristics in their power spectra as the CoMP waves. Evidently, p-modes contain orders of magnitude more power than required for coronal heating. The physical mechanism proposed to explain the ubiquity of these waves is the double mode conversion process of p-modes during their propagation across the low atmospheric layers, during which their energy is transferred to Alfvénic modes (Cally and Hansen, 2011; Felipe, 2012; Cally, 2017). A strong consequence of this is
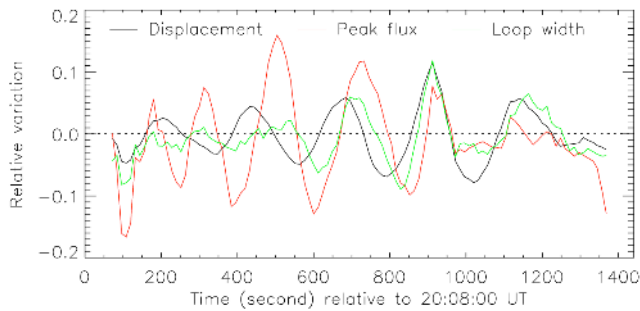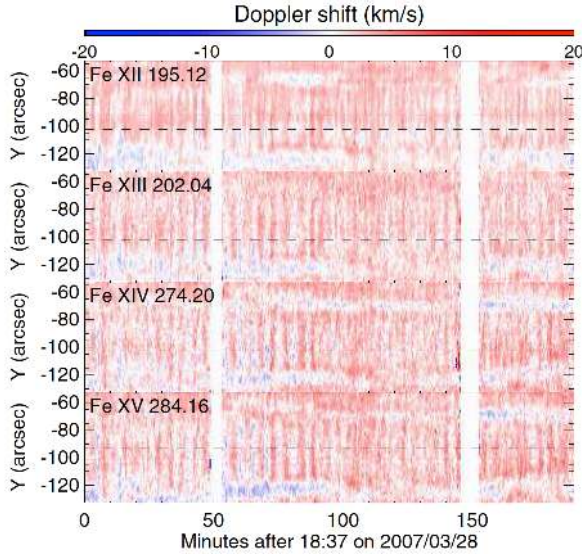
**Fig. 3** Decayless oscillations of coronal loops seen in the loop displacement, peak flux and loop width estimated from the AIA 171 Å images. Adapted from Wang et al. (2012).

that solar and stellar coronae have a non-negligible energy source in their internal acoustic oscillations. Although direct observations of this process are still lacking, these results also suggest that p-modes may play a role in the onset of standing or propagating Alfvénic modes.

### 2.3 Decayless oscillations

Decayless oscillations normally refer to standing waves without obvious observed damping in coronal loops. In coronal lines[1], these oscillations were first reported independently by Wang et al. (2012) and Tian et al. (2012) through imaging and spectroscopic observations, respectively. The transverse oscillations reported by Wang et al. (2012) from SDO/AIA observations appear to be triggered by a coronal mass ejection. They lasted for more than ten cycles and even revealed growing amplitudes (Figure 3). Tian et al. (2012) performed a survey of decayless (referred to as "persistent" in their paper) Doppler shift oscillations using three-month spectroscopic observations from the EUV Imaging Spectrometer (EIS, Culhane et al., 2007) on board Hinode. They found that such decayless oscillations, with a period of 3–6 minutes and a velocity amplitude of 1–2 km s$^{-1}$, are very common in quiet coronal loops and can be observed in several coronal emission lines formed in the temperature range of 1.3–2 MK (Figure 4). These oscillations generally reveal no obvious damping during the whole observed time interval, which often last for a few hours. They were interpreted as standing kink oscillations by these authors. Since 2012, these decayless oscillations have been frequently reported for a variety of different observations (e.g., Nisticò et al., 2013, 2014), and it was found that their periods scale with the loop length (Anfinogentov et al., 2015), strongly supporting the standing wave interpretation.

---

[1] Small amplitude decayless oscillations were also observed in a prominence with *Hinode*/SOT (Ning et al., 2009), and of significant and increasing amplitude in a coronal loop with rain (Antolin and Verwichte, 2011). Due to the presence of chromospheric material and the associated processes specific to the formation of prominences and coronal rain, the processes responsible for such oscillations may likely be different than those observed in coronal lines.

**Fig. 4** Decayless oscillations of quiet coronal loops seen in the Doppler shift of four coronal emission lines. The Y-axis is roughly aligned with the corona loop. Adapted from Tian et al. (2012).

The decayless behavior of these waves suggests a continuous supply of energy to the system. Several different ideas have been proposed to maintain these decayless or persistent oscillations. For instance, Nakariakov et al. (2016) interpreted these decayless kink oscillations as a self-oscillatory process (a process in which the driver is a consequence of the oscillation itself, see Jenkins, 2013), driven by interaction between the loops and quasi-steady flows at the loop footpoints. Antolin et al. (2016) have shown that the decayless pattern could also be an apparent effect produced by the combination of low instrumental resolution and the periodic brightening generated by TWIKH rolls (Transverse Wave Induced Kelvin-Helmholtz rolls, cf. Sec. 3.3). In this interpretation, the decayless character reflects the low damping character of the azimuthal Alfvén waves resonantly coupled to the kink mode at the boundary layer. Another theory is through continued footpoint driving (Karampelas et al., 2017) providing an upward Poynting flux balancing the resonant and non-linear damping of the kink waves. Recent numerical experiments (Karampelas et al., 2019b; Guo et al., 2019b) reproduce the observations of decayless oscillations very well. More recently, Afanasyev et al. (2020) developed a one-dimensional and time-dependent analytical model by considering kink oscillations of coronal loops driven by random motions of loop footpoints. They have managed to reproduce a number of observational facts about these decayless kink oscillations, such as the quasi-monochromaticity, period-length relationship and excitation of multiple harmonics.

2.4 Available energy in quasi-periodic fast mode wave trains

The high cadence and spatial resolution of SDO/AIA in EUV enabled the discovery of quasiperiodic fast mode propagating wave trains (QFPs) (see, Liu et al. (2010, 2011), the review Liu and Ofman (2014). The waves were observed to be associated with flares and propagate at a high speed of 1000-2000 km s$^{-1}$ with periods in the range of minutes and intensity variations $\delta I/I \sim 5\%$. The waves were modeled first by Ofman et al. (2011) using a 3D MHD model of a realistic bipolar active region structure and identified as fast-mode magnetoacoustic waves. Since the initial discovery, these waves were observed, studied, and modeled in many events associated with flares (see, e.g. Liu et al., 2012; Shen and Liu, 2012; Shen et al., 2013, 2017, 2018; Yuan et al., 2013; Kumar and Manoharan, 2013; Nisticò et al., 2014; Zhang et al., 2015; Goddard et al., 2016b; Qu et al., 2017; Ofman and Liu, 2018). Evidently, the QFPs carry some of the energy flux produced by the flares, and the observed dissipation of the QFP waves should result in coronal heating. The energy flux of the waves was estimated first using the parameters observed by SDO/AIA on 2010/08/01 by Liu et al. (2011) and was found to be in the range $(0.1 - 2.6) \times 10^4$ W m$^{-2}$, which is of the same order as the steady-state heating requirement of active region loops. The QFP wave energy flux estimate was based on the WKB approximation given by $E = \rho \delta v^2 v_{ph}/2 \geq \rho(\delta I/I)^2 v_{ph}^3/8$ (Aschwanden, 2004), where the intensity of the line emission, $I \propto \rho^2$, and the phase speed $v_{ph}$ were determined directly from SDO/AIA observations ($v_{ph} = 1600$ km s$^{-1}$), and the number density is taken to be the typical coronal electron density $\sim 10^8$ cm$^{-3}$. The QFP wave trains lasted on the order of $\sim 0.5$ hr and were repeatedly produced in the 2010/08/01 event. However, the divergence of the magnetic funnel in the active region and apparent dissipation of the waves reduced the apparent energy flux away from the flaring source.

Ofman et al. (2011) used the 3D MHD model results in an idealized bipolar active region of QFP wave trains combined with the WKB approximation to estimate the energy flux as $E = \rho \delta v^2 V_f/2 = 3.7 \times 10^5$ W m$^{-2}$, where $\rho$ is the coronal density, $\delta v$ is the wave velocity amplitude, and $V_f$ is the fast magnetoacoustic speed. The model energy flux was an order of magnitude greater than the direct estimate by Liu et al. (2011). However, the model estimate was based on idealized AR parameters in qualitative agreement with observations. In a recent study by Ofman and Liu (2018) of the double QFP event observed by SDO/AIA on 2013-5-22 the lower limit of the wave energy flux was estimated as $1.8 \times 10^2$ W m$^{-2}$ high in the corona. The authors concluded that, taking into account coronal loop expansion, the wave energy flux could be at least one to two orders of magnitude higher near the source of the QFPs.

Statistical study of QFP waves indicates that these waves are quite common and often observed to be associated with C-class flares, although they can also result from stronger and weaker flares (Liu et al., 2016). Thus, combined with the challenging detection of these waves for lower energy flares, the contribution of QFP wave trains to coronal heating and to the energy flux requirement may be more significant than initially estimated. Thus, the problem of QFP wave train heating parallels the coronal heating problem by flares, where small energy flares (i.e., undetected nanoflares) are required for coronal heating and possibly their associated QFP waves are not directly detected (Aschwanden, 2004).

2.5 Observations and energy estimates of MHD waves in the lower solar atmosphere

The lower solar atmosphere (photosphere and chromosphere) plays an important role in the transmission of wave energy from the solar interior to the corona. Therefore, the assessment of wave energy content in this layer is crucial in understanding the coronal heating problem. Moreover, it is well established that the solar chromosphere requires substantially more energy flux than the corona ($10^3$–$10^4$ W m$^{-2}$) to compensate for its huge radiative losses (Withbroe and Noyes, 1977).

Recent observational findings from high-resolution ground (e.g., 1m-Swedish Solar Telescope, ROSA – Rapid Oscillations in the Solar Atmosphere) and space-based (e.g., IRIS – Interface Region Imaging Spectrometer, SDO – Solar Dynamics Observatory) observations reveal the presence of a high amount of energy flux associated with different MHD modes in a variety of magnetic structures coupling the various layers of the solar atmosphere.

In the photosphere, wave behaviour is found in pores and sunspots. Jess et al. (2009) reported the detection of Alfvén waves with periods of the order of 126-400 s associated with a large bright-point group. The energy flux associated with these wave modes is found to be $1.5 \times 10^4$ W m$^{-2}$ in the chromosphere, which partially fulfills the chromospheric energy requirements. Using that 1.6% of the solar surface is observed to be covered by bright-points and assuming that they support such torsional waves with a 42% transmission coefficient (which may be on the high side), Jess et al. (2009) have estimated the global average energy in the corona as 240 W m$^{-2}$, which is sufficient to heat it locally.
Grant et al. (2015) have detected upwardly propagating slow sausage waves in magnetic pores, which initially carry an energy flux of $3.5 \times 10^4$ W m$^{-2}$. The sausage wave energetics show a substantial decrease up to the chromosphere. These observations make it evident that magnetic pores transport waves to the higher layers, while also releasing energy in the local chromospheric plasma. However, it is not well quantified how much wave energy undergoes mode conversion, reflection or refraction. Aside from the frequently observed sausage modes, higher order magnetoacoustic oscillations ($m \geq 1$) have also been observed in photospheric waveguides (e.g. Jess et al., 2017; Stangalini et al., 2018, and references cited there), including body and surface modes (Keys et al., 2018). Furthermore, Grant et al. (2018) presented evidence of Alfvén wave heating of the chromospheric plasma in an active region sunspot umbra. They showed the presence of mode conversion and the formation of magnetoacoustic shocks.
In conclusion, the random buffeting motions in the photosphere generate many MHD modes in the photospheric magnetic flux tubes along with a sufficient amount of energy flux. However, one has to bear in mind that these magnetic flux concentrations constitute only a small part of the photosphere, and it is unclear if these wave motions also propagate to the corona in quiet regions, where such photospheric magnetic flux tubes are less prevalent.

In the chromosphere, magnetic structures play a major role in guiding MHD waves. They are thus the prime structures in which waves are detected. In particular, Fig. 5 displays the results of Morton et al. (2012) who have observed the simultaneous presence of fast kink and sausage waves in mottles and fibrils using ROSA H$_\alpha$ observations, and found that they carry an average energy of respec-
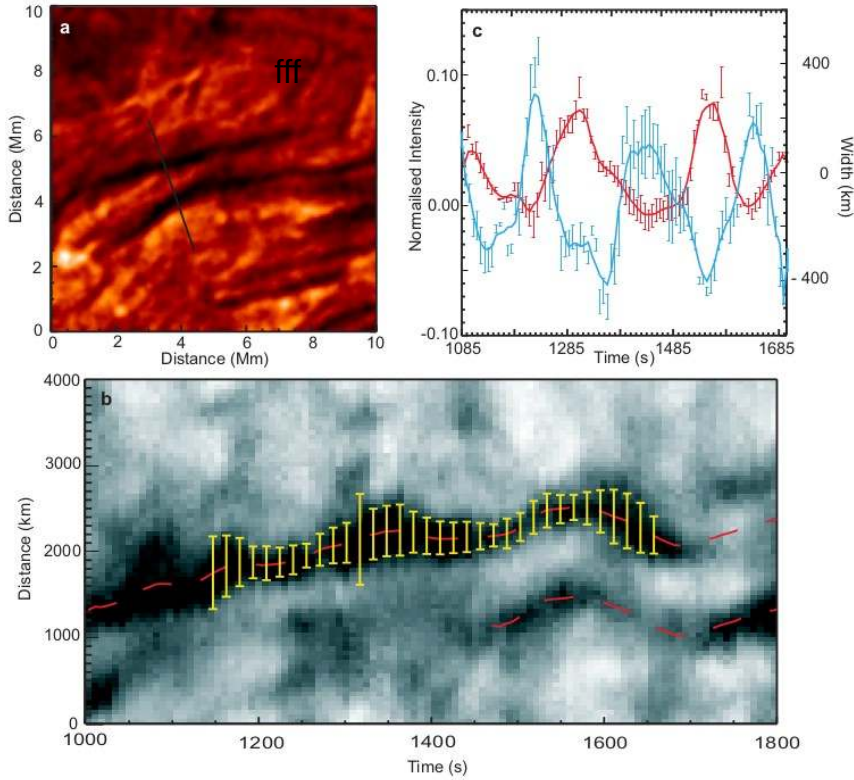
**Fig. 5** Simultaneous wave modes in a chromospheric magnetic flux tube using ROSA $H_\alpha$ observations. Time-distance map ('b') exhibits the displacement of the tube's axis (red-dotted line) as a whole (kink waves), while its cross-section variation (sausage wave) is depicted by the yellow bars measuring the variation of tube's width. All measurement is done by Morton et al. (2012) from where this figure is adopted and displayed here. Kink wave respectively have period, upward propagation velocity, amplitude, and energy flux as $\sim$232 s, $\sim$71 km s$^{-1}$, $\sim$5 km s$^{-1}$, 4300 W m$^{-2}$. While, the same for the observed sausage wave are given respectively as $\sim$197 s, $\sim$67 km s$^{-1}$, $\sim$1-2 km s$^{-1}$, 11700 W m$^{-2}$

tively 4300 W m$^{-2}$, and 11700 W m$^{-2}$, once again stressing the large amount of energy present in the lower atmosphere.

Going from the chromosphere to the transition region, spicules and their TR counterparts show ample evidence of wave dynamics. Observations of swaying motions in spicules with high-resolution imaging instruments such as *Hinode*/SOT and IRIS have long been attributed to propagating Alfvénic waves (De Pontieu et al., 2007; Tian et al., 2014). The amplitudes of the swaying motions are usually of the order of $10 - 25$ km s$^{-1}$, although a factor of 5 larger motions have also been observed (Antolin et al., 2018b). In general, 1 or 2 oscillations of the spicules can be captured before the structure disappears, and a wide range of reported periods of $100 - 500$ s and also high-frequency ($20 - 50$ s Okamoto and De Pontieu, 2011). Srivastava et al. (2017) showed the ubiquitous presence of high frequency ($\approx$12–42 mHz) torsional motions in spicular-type structures in the chromosphere
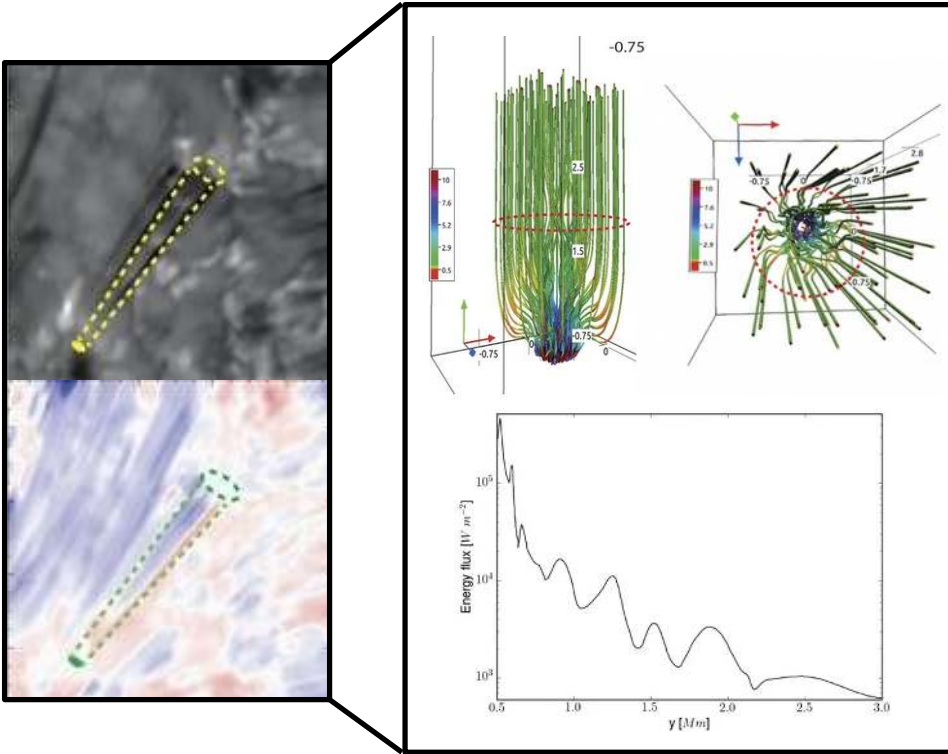
**Fig. 6** The spicular-type structure (top panel of the left-box) shows periodic reversal of the velocity (snapshot shown in the bottom-panel of the left-box) indicating the presence of torsional Alfvén wave. The numerical simulation (top-panel of the right-box) exhibits similar torsional motions in the model fluxtube, that carry substantial energy (bottom-panel of the right-box) through the solar chromosphere, TR, and corona (Credit: Srivastava et al., 2017).

(Fig. 6, left box). Their numerical model showed that these observations resemble torsional Alfvén waves associated with high frequency drivers containing a huge amount of energy ($\approx 10^5$ W m$^{-2}$) in the chromosphere (Fig. 6, right-panel). It is important to note, however, that the observational signatures of TWIKH rolls can also explain these observations (Antolin et al., 2018b). Even after partial reflection from the transition region, Srivastava et al. (2017) found that a significant amount of energy ($\approx 10^3$ W m$^{-2}$) is being transferred into the overlying corona, which is sufficient to compensate the coronal radiative losses (Fig. 6, right panel). The propagation speeds of waves in spicules are often difficult to measure, due to their short lifetimes, the combination of (upward/downward) propagating and standing waves (Okamoto and De Pontieu, 2011) and also due to the rapidly increasing Alfvén speed at the observing heights. On average, speeds of $200 - 300$ km s$^{-1}$ are reported in these works.

The swaying motions of spicules suggest a transverse displacement of a waveguide and therefore such motions are often interpreted as kink waves. However,

caution is required when only imaging information is available, since torsional Alfvén waves may also produce strand-like, swaying structures such as spicules (Antolin et al., 2018b). Moreover, additional to the swaying, torsional and longitudinal motions are observed in spicules (De Pontieu et al., 2012; Sekse et al., 2013), and are likely strongly connected to their generating mechanisms and to the nature of the wave. The nature of the Alfvénic wave (kink or torsional Alfvén wave) is important when trying to estimate the energy flux carried by the wave, since the collective or local nature distributes the wave energy differently across the waveguide (Van Doorsselaere et al., 2014). Assuming a filling factor of 1 (a best case scenario), a typical spicule mass density of $8-16 \times 10^{-14}$ g cm$^{-3}$ and based on the reported values, one can estimate the energy flux in swaying spicules as $0.1-3 \times 10^3$ W m$^{-2}$, with the strongest cases at $1-4 \times 10^4$ W m$^{-2}$. Usually, 3% of the energy is assumed to enter the corona, leading to average energy flux values of 100 W m$^{-2}$ available for coronal heating, which is sufficient for the quiet Sun and for the acceleration of the solar wind (Tian et al., 2014).

2.6 Heating function assessment by slow waves

The presence of waves in the solar atmosphere may not only provide energy for heating the corona, but could also provide us with a tool to seismologically estimate the coronal heating function and the related dissipation coefficients, such as thermal conduction and viscosity (see the review by Wang et al., 2021, this issue). Here we forego that, more importantly, even the most basic property of the magnetized coronal plasma such as the magnetic field strength needed for any magnetically based heating function estimate is difficult to determine directly, and in some cases can only be estimated from coronal seismology. However, we keep this subject for the review of Nakariakov et al. (2021), this issue.

   The impact on the dynamics of MHD waves of thermodynamic activity of the corona, i.e. processes of its continuous cooling via the optically thin radiation and thermal conduction, and resupply of energy by some yet unknown heating mechanism, was recently investigated by Nakariakov et al. (2017); Claes and Keppens (2019); Kolotkov et al. (2019, 2020). This allows for developing a new approach for a remote diagnostics of thermodynamic properties of the corona, including processes of its cooling and heating, by coronal seismology. For example, additional restrictions on the coronal heating mechanism can be obtained via accounting for perturbations of the thermal equilibrium of the corona by compressive, e.g. slow magnetoacoustic, waves. Indeed, assuming the plasma heating and cooling processes are some different functions of the plasma thermodynamic parameters, i.e. density and temperature, and potentially of the magnetic field too, both of them can be perturbed by the waves. Such a wave-caused destabilisation of the initial thermal equilibrium leads to the onset of a *heating/cooling misbalance* acting as an additional natural mechanism for the energy exchange between the plasma and the wave.

   Kolotkov et al. (2019) showed that it is convenient to use specific thermal misbalance time scales $\tau_1$ and $\tau_2$ connected to the rates of change of the net energy gain $H(\rho, T)$, and loss $L(\rho, T)$ including radiative cooling and field-aligned thermal conduction, through the function $Q(\rho, T) = L - H$ with the plasma density $\rho$ and temperature $T$, $Q_T \equiv (\partial Q/\partial T)_\rho$ and $Q_\rho \equiv (\partial Q/\partial \rho)_T$, as $\tau_1 = \gamma C_{\mathrm{V}}/[Q_T - (\rho_0/T_0)Q_\rho]$
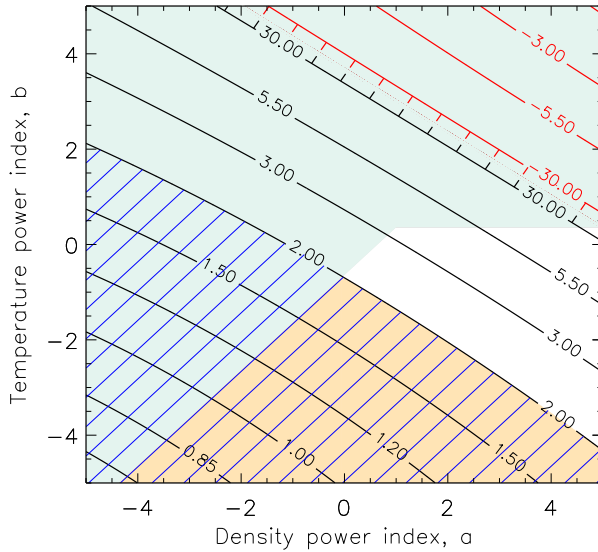
**Fig. 7** Dependence of the oscillation quality factor $q$ on the density and temperature power indices used for parametrising the heating function as $H(\rho, T) \propto \rho^a T^b$, for the following values of the equilibrium parameters of the plasma: $T_0 = 6.3 \times 10^6$ K, $\rho_0 = 10^{-11}$ kg m$^{-3}$, loop length $L = 180 \times 10^6$ m, Spitzer conductivity $\kappa = 10^{-11} T_0^{5/2}$ W m$^{-1}$ K$^{-1}$, mean particle mass $m = 0.6 \times 1.67 \times 10^{-27}$ kg, $k_B = 1.38 \times 10^{-23}$ m$^2$ kg s$^{-1}$ K$^{-1}$, and $\gamma = 5/3$. The black and red contours show the regimes of damping (positive $q$) and amplification (negative $q$), respectively. The blue-shaded region shows values of $a$ and $b$ where the time scales of the heating/cooling misbalance $\tau_1$ and $\tau_2$ become negative, for which other thermal instabilities may occur (see Field, 1965). The hatched region shows values of $q < 2$ for slow-mode oscillations detected in observations (Nakariakov et al., 2019). The yellow-shaded region outlines heating models which are stable to thermal instability and for which $q < 2$. Figure modified from Kolotkov et al. (2019).

and $\tau_2 = C_V/Q_T$ with $C_V$ being the specific heat capacity. With this, the dispersion relation for linear slow waves describes the evolution of two acoustic and one thermal (entropy-related) modes. The 3rd order dispersion relation can be solved numerically for the real, $\omega_R$, and imaginary, $\omega_I$, parts of a complex frequency $\omega$, while allowing the value of $\omega_I$ to be comparable to $\omega_R$. The *q-factor* (also known as quality factor) is computed as $q = \tau_D/P$, using the oscillation period $P = 2\pi\omega_R^{-1}$ and damping time $\tau_D = \omega_I^{-1}$.

Using the radiative cooling $L(\rho, T)$ from the CHIANTI atomic database (Dere et al., 1997, 2019), and a parametrised heating function $H(\rho, T) \propto \rho^a T^b$, Kolotkov et al. (2019) compute numerically the oscillation quality factor $q$ as a function of the heating indices $a$ and $b$. The results are displayed in Fig. 7 for different values of the heating power indices $a$ and $b$ and for the equilibrium parameters corresponding to hot and dense post-flare coronal loops. Direct comparison of the values of $q$ shown in Fig. 7 with those usually seen in observations of slow magnetoacosutic oscillations of coronal loops (see e.g. Nakariakov et al., 2019, for the most recent statistical survey) by e.g. SOHO/SUMER and Yohkoh/BCS,
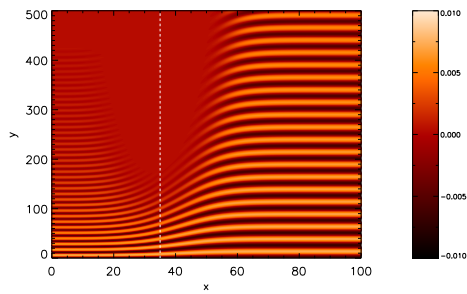
**Fig. 8** Snapshot of Alfvén wave velocity component out of the plane, for a periodic driver on the bottom boundary. The figure displays the turning of the wave fronts due to phase mixing in the middle region with the largest variation of the Alfvén speed, and the associated phase mixing damping in the region where the turning is the strongest, is indicated with the vertical white dashed line. Figure taken from McLaughlin et al. (2011).

shows that the heating models with $a$ and $b$ approximately delineated by a triangle with vertices $(-3.5, -4)$, $(0, -0.5)$, and $(5, -4)$ in Fig. 7, excluding the regions of the thermal mode instability, could be responsible for the observed rapid damping of slow waves in the corona (Wang, 2011). Thus, the proof-of-concept of Kolotkov et al. (2019) show that slow waves can indeed serve to put limits on (power indices of) the coronal heating function.

The discussed misbalance between heating and cooling processes in plasma can cause additional phase shifts between density and temperature perturbations in slow waves, thus affecting, for example, estimates of the effective polytropic index. In particular, Zavershinskii et al. (2019) demonstrated analytically that the polytropic index, a coefficient linking the slow wave phase speed with the plasma temperature, can vary non-monotonically with temperature due to the effect of the thermal misbalance, so that it deviates from the adiabatic value 5/3 to 1.4-3.2. This can be a natural cause for higher values of the polytropic index at hotter plasma temperatures observed by Krishna Prasad et al. (2018), that cannot be explained by the classical Spitzer thermal conduction. Implication of these theoretical results for probing the corona is a promising future research avenue.

## 3 Models

### 3.1 Phase mixing models

As already pointed out by Cowling (1953) and Piddington (1956), classical resistive or viscous dissipation of the Alfvén wave energy is not efficient in a homogeneous magnetized plasma and this slow dissipation rate remains a key obstacle in more advanced present day wave-based heating models (see e.g. Arregui, 2015; Cargill et al., 2016). The main problem is to rapidly transfer the wave energy from large to small length scales, where (classical) dissipation is effective. The concept of phase mixing as described by Heyvaerts and Priest (1983) aims to enhance this dissipation rate through the creation of small length scales in an inhomogeneous medium. Phase mixing occurs when a local gradient in the Alfvén speed is present; as waves propagate along field lines with different Alfvén speeds, the wave front

turns and the waves become increasingly out of phase. This is shown graphically in Fig. 8, displaying results of McLaughlin et al. (2011). This process generates increasingly smaller length scales (across the background magnetic field) and hence, more efficient dissipation. Although resonant absorption and phase mixing are often discussed as individual mechanisms, there is a natural link between these mechanisms, as both rely on the presence of a variation in the local Alfvén speed profile (Soler and Terradas, 2015). Hence, the small-scale oscillations in the resonant layer will naturally undergo phase mixing due to local variation in the Alfvén speed (see e.g. Ruderman et al., 1997a,b). However, the damping caused by phase mixing depends on the actual value of the resistivity, while the damping of resonant absorption does not (as resonant absorption itself is an ideal process). An extensive body of literature on both resonant absorption and phase mixing exist, for which we refer the interested reader to reviews by e.g. Aschwanden (2004); Goedbloed and Poedts (2004); Goossens et al. (2011).

Most theoretical (including computational) studies of phase mixing start from an equilibrium setup where a pre-existing profile in the Alfvén speed is present. Most often, this setup consists of a uniform background magnetic field, where a gradient in the density is balanced by a temperature variation to maintain pressure balance. Waves are then considered as perturbations of this equilibrium or injected through boundary driving. The process of phase mixing will lead to the most efficient dissipation of the Alfvén waves (and hence strongest heating) where the gradient in the density (Alfvén speed) profile is steepest.

The self-consistency of heating by phase mixing of Alfvén waves was investigated in more detail by Cargill et al. (2016) by analysing the evolution of the density profile. These authors showed that although phase mixing increases the efficiency of the wave energy dissipation where gradients in the local Alfvén speed occur, the resulting heating in this basic model cannot self-consistently sustain the required density profile in closed loops. As the local density in closed loops is related to the magnitude of the heating (see e.g. Klimchuk, 2006; Reale, 2014), the phase mixing heating profile is not consistent with the heating profile to sustain the density profile. Cargill et al. (2016) also investigated whether feedback of the heating on the density profile through evaporation would be able to modify the local density (see also Ofman et al., 1998). Although some local structuring of the density profile occurred, it only happened on timescales longer than the cooling and draining timescales and hence, does not help address the efficiency problem of wave-heating. In addition, the authors point out that transport coefficients need to be substantially enhanced to obtain effective heating in the first place. Using MHD simulations including thermal conduction and optically thin radiation, Van Damme et al. (2020) for the first time modelled the feedback process through evaporation entirely self-consistently (i.e. without the use of scaling laws) and also found that Alfvén wave phase mixing only leads to modest heating in the shell regions of the loop, where the mass increase through evaporation is not sufficient to modify the phase mixing process.

If the imposed density structure is not compatible with the heating profile resulting from phase mixing, how then is this assumed equilibrium structure supported? Is an alternative heating mechanism present that is compatible with the density structuring? And if so, does that immediately imply that the wave-based heating (through phase mixing) is comparatively small?

In addition to requiring the presence of a variation in the local Alfvén speed profile, the phase mixing model as it was originally introduced by Heyvaerts and Priest (1983) implies the presence of an ignorable coordinate, a setup which might not be representative of the highly inhomogeneous solar atmosphere (Parker, 1991; Ofman and Davila, 1995), although approximately similar conditions may occur in coronal holes.

Pagano and De Moortel (2017) investigated the heating by phase mixing in a 3D numerical model of a boundary-driven flux tube. The flux tube is modelled as a cylindrical density enhancement in a uniform magnetic field and transverse displacements of the footpoint of the cylinder generate kink modes which, as they propagate along the flux tube, couple to azimuthally polarised Alfvén modes in the boundary shell of the cylindrical flux tube. Due to the density gradient in the inhomogeneous boundary layer, the Alfvén waves phase mix but, even using (excessively) large values of magnetic resistivity and large-amplitude footpoint driving, the heating due to phase mixing was found to be insufficient to be relevant for coronal heating (i.e. to balance the expected losses through radiation and conduction), a conclusion similar to the remark made by Cargill et al. (2016) about the need to substantially enhance transport coefficients. By varying parameters such as the length of the non-uniform layer, the density structure, and the persistence of the driver, Pagano and De Moortel (2017) find that phase mixing of these propagating waves leads to temperature increases of the order of $10^5$K or less, a figure that is in agreement with the analytical estimate by Terradas and Arregui (2018), even though these were for standing waves.

When simulations are performed using 3 observed coronal loop oscillation harmonics as input, Pagano et al. (2018) found that the presence of these multiple harmonics causes drifting of the location of the heating. Still, the mechanism did not seem to provide enough energy to maintain the full thermal structure constrained by the observed coronal properties, and the multiple harmonics inhibited the formation of small scales. Pagano and De Moortel (2019) included an observed spectrum of transverse waves, using a boundary driver which consists of a series of 1000 superimposed random pulses was used drawn from a reconstructed spectrum. The results again indicate that it is unlikely that phase mixing of Alfvén waves generated by the observed power spectrum heats coronal loops, although, the waves could be important in the generation of small scales.

## 3.2 Alfvén wave heating models

### 3.2.1 Alfvén wave induced shock heating

Alfvén waves have long been particularly attractive coronal heating candidates due to their ability to carry large amounts of energy throughout the solar atmosphere (Alfvén, 1947; Uchida and Kaburaki, 1974) and can potentially also lead to solar wind acceleration (Hollweg, 1990; Ofman, 2010). The Poynting flux upward from convective motions in magnetic concentrations at photospheric level is expected to be on the order of $10^6$ W m$^{-2}$ (Parnell and De Moortel, 2012), although the strong magnetic expansion in the upper layers leads to an effective Poynting flux of $10^4$ W m$^{-2}$ into the chromosphere. The ion-neutral friction due to the partial ionisation of the plasma in the chromosphere strongly damps the Alfvén waves,

in particular the high-frequency spectrum. Combined with reflection, these effects lead to only a $1-3\,\%$ effective transmission rate into the corona (Soler et al., 2017, 2019), similar to estimated footpoint leakage of coronal waves (De Pontieu et al., 2001). Overall, the energy budget from torsional Alfvén waves generated in the photosphere is estimated to be on the order of $10^2\ \mathrm{W\,m^{-2}}$ in the corona, which is just enough for the quiet Sun or coronal hole. The double mode conversion process from p-mode waves into Alfvénic waves in the chromosphere and transition region is expected to contribute similar energy rates (Morton et al., 2019).

Various models for Alfvén wave propagation in the solar atmosphere have a different nature depending on the region and wave guide under consideration. The geometry of the waves has been selected to be either planar (a.k.a linear, e.g., Suzuki and Inutsuka, 2005; Murawski and Musielak, 2010) or azimuthal (a.k.a. circular, e.g., Zhugzhda, 1996; Vasheghani Farahani et al., 2010; Wójcik et al., 2017). For instance Alfvén wave propagation of waves with linear polarisation may be more appropriate in the relatively diffuse coronal holes, while the circular polarisation may be more applicable for the propagation in structures showing strong density contrast, such as solar jets, spicules, tornadoes, and loops (Vasheghani Farahani et al., 2011).

Alfvén waves need an efficient dissipation mechanism in order to play a dominant role in coronal heating. A first successful dissipative model was based on nonlinear mode conversion of these waves into compressive modes (evolving into shocks) due to the flux tube expansion (and associated centrifugal force) and the ponderomotive force (Hollweg et al., 1982; Lau and Siregar, 1996; Ofman and Davila, 1998; Antolin and Shibata, 2010). This idea has persisted through the decades thanks to the accompanying ability to generate spicule-like excursions of material into the corona (Kudoh and Shibata, 1999; Matsumoto and Shibata, 2010; Arber et al., 2016; Brady and Arber, 2016) and accelerate the solar wind (Matsumoto and Suzuki, 2014; Suzuki and Inutsuka, 2006). Furthermore, this model has demonstrated that waves can lead to small nanoflare-like intensity bursts during dissipation (Moriyasu et al., 2004; Antolin et al., 2008), thus placing caution when interpreting observations of these events or associating the nanoflare term solely to reconnection-based models. Although highly self-consistent in its ability to explain various features of the solar atmosphere, this model relies on the presence of density fluctuations, and sufficiently large transverse wave fluctuations (compared to the local Alfvén speed) for the relevant nonlinear effects to become important. A natural question is whether this matches observations and the answer yet unknown. Parker Solar Probe does indicate, however, that the density fluctuations in the open corona is far greater than previously thought (Bale et al., 2019).

A well established model is that of Suzuki and Inutsuka (2005) who describe the propagation of a low frequency Alfvén wave in coronal holes from the photosphere to an altitude of 0.3AU. The granular motion of the photosphere results in steady transverse motions perturbing the magnetic field lines and exciting Alfvén waves (Cranmer and van Ballegooijen, 2005). The 1D model provided by Suzuki and Inutsuka (2005) resembles a superradial open magnetic flux tube conserving magnetic flux, where the expansion is a two step superradial function with the use of two expansion factors. Their choice for a two step superradial function was due to the height dependence of the magnetic field strength reconstructed by Tu et al. (2005). They included the effect of field line curvature, radiative cooling and
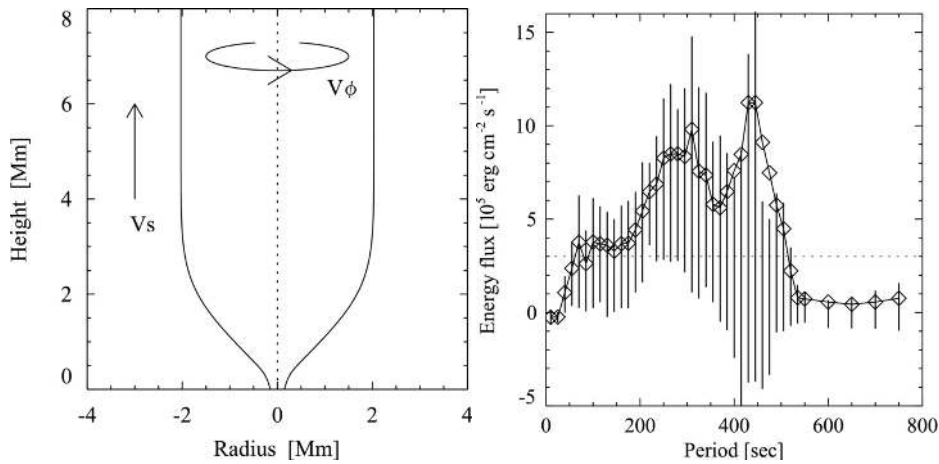
**Fig. 9** Left: Sketch on the configuration of Alfvén wave heating models. Right: Alfvén wave energy flux as a function of period. The figures are taken from Matsumoto and Shibata (2010).

thermal conduction in the MHD equations. The solutions to these MHD equations enabled Suzuki and Inutsuka (2005) to compute the variations of the radial and tangential speeds together with the temperature and density as a function of altitude (see Fig. 9 for a sketch of the configuration). The results proved adequate for atmospheric heating due to two effects; the first stage of heating is due to the dissipation of low frequency Alfvén waves mainly heating the inner solar atmosphere, while the second stage of heating is due to the induction of compressive perturbations (especially slow waves) due to the nonlinear efects connected with the Alfvén wave propagation that causes wave steepening ending up in shock formation that mainly contributes towards coronal heating. The nonlinear effects connected with outward propagating Alfvén waves that experience shocks contributes in two ways; the first aspect is the heating due to the increase of wave amplitudes that is confirmed by the non-thermal broadening of the emission lines, the second aspect is the creation of shocks which rapidly dissipates the waves. The contribution of the second aspect towards heating is greater than the first aspect (Nakariakov et al., 2000). As a matter of fact, the efficiency of damping and hence heating due to low frequency Alfvén waves also depends on the activity of the region. In particular, the damping of surface Alfvén waves occurs on a shorter scale in active regions compared to quiet solar regions. This means that in quiet regions, the surface Alfvén wave is able to contribute towards heating the corona at higher altitudes (Evans et al., 2009). In addition, the period of the Alfvén wave itself is key in determining its contribution to coronal heating. This statement is backed by the simulations of Matsumoto and Shibata (2010) where nonlinear Alfvén waves were driven by photospheric convection towards the transition region in the presence of gravity and empirical chromospheric cooling. Their model showed that the region bounded between the photosphere and the transition region acts as a resonant cavity, a fact that has been recently observed above sunspots for the first time (Jess et al., 2019). It can be readily noticed from the right panel of Fig. 9 that waves with periods between 100 s to 500 s are able to transport flux to the corona, and that the maximum energy flux is carried when the period of the Alfvén wave

is around 400s coinciding with the resonant frequencies in the cavity (Matsumoto and Shibata, 2010).

Coronal resonances of Alfvén wave propagating in solar loops have also been reported in the model proposed by Antolin and Shibata (2010). The loop is a gravitationally stratified semitorus, with magnetic field expansion, similar to the left panel of Fig. 9. The advantage of this model is that it sheds light on the efficiency of heating taking into account the loop geometry in which Alfvén waves propagate. This enabled Antolin and Shibata (2010) to state that Alfvén waves provide efficient and uniform heating when propagating in thick loops where the area expansion between the photosphere and corona is greater than 2.5 orders of magnitude with lengths at least as long as 80 Mm. Since in the solar quiet regions the loops are both longer and wider compared to loops in active regions, the efficiency of Alfvén wave heating in quiet solar regions is more pronounced compared to active regions. Regarding the period of the waves, Antolin and Shibata (2010) concluded that the shocks connected with long-period waves increase the average temperature of the corona, while shocks connected with short-period waves are unable to further heat the corona despite being more numerous (Suzuki and Inutsuka, 2006). The short-period waves are only just strong enough to maintain the coronal temperature. Heating by the resonance cavity with a monochromatic driver matching the eigenfrequency of the loop was found to lead to temperatures close to 5 MK, but the loops were not in a state of thermal equilibrium.

Regarding the contribution of the compressive shocks towards coronal heating, Matsumoto (2016) stated that shock compressive heating is very efficient below the altitude of 4 Mm, while above this height the incompressive heating due to direct dissipation of magnetic and velocity shear in Alfvén waves is dominant. Moreover, Matsumoto and Suzuki (2014) showed that these chromospheric compressive shocks generate curved wedge shaped Alfvén waves, which could play a role in heating the higher layers. Thus, the back reaction of the induced compressive perturbations on the Alfvén wave results in Alfvén wave shocks that also contribute towards coronal heating. The induced compressive perturbations are due to the nonlinear forces connected with Alfvén waves, namely the magnetic tension, centrifugal, and ponderomotive forces. It is worth noting that the ponderomotive coupling of Alfvén waves to slow modes creates shocks that dominates the heating due to resistive dissipation (Arber et al., 2016; Brady and Arber, 2016). The non-linear behaviour of Alfvén waves was described by e.g. Suzuki (2008); Vasheghani Farahani et al. (2011); Suzuki (2012); Vasheghani Farahani and Hejazi (2017). In particular, Vasheghani Farahani et al. (2012) implemented the second order thin flux tube approximation (Zhugzhda, 1996) and studied the parallel nonlinear cascade of torsional and shear Alfvén waves in open magnetic fields. They showed that the shock formation for shear Alfvén waves comes into play earlier than torsional waves in the lower solar atmopshere.

Another mechanism playing a role in chromospheric heating is Ohmic diffusion and ion-neutral collisions which strongly affects torsional Alfvén waves during their propagation in the chromosphere (Soler et al., 2019; Wójcik et al., 2020) and leads to heating. In any case, the chromosphere plays a crucial role for coronal heating, because of the resulting evaporation of material due to coronal heating and thus providing the mass source. The localised heating could result in thread structuring in the corona (Copil et al., 2008), which is in contradiction with the recent results of Cargill et al. (2016); Van Damme et al. (2020).

*3.2.2 Alfvén wave turbulence heating*

Turbulent heating models have gained popularity recently in the context of coronal heating (see the review by Bruno and Carbone, 2013, of this mechanism in the solar wind context). However, there is still no direct evidence that the corona is turbulent. This might change in the near future thanks to the Parker Solar Probe, which could confirm turbulence at heights around or below the Alfvén critical point. Still, the non-thermal broadening of the coronal spectral lines could already be indicative of turbulent fluctuations (Banerjee et al., 1998; Singh et al., 2006; Hahn and Savin, 2013, 2014). More indirect evidence is present in the CoMP observations through the measurement of a $1/f$ spectrum in closed loops (Morton et al., 2016, 2019). Turbulent heating models are best categorized as wave or alternative-current (AC) mechanisms in the limit of weak turbulence, as the turbulent energy cascade is thought to be generated by nonlinear (self) interactions of waves. The underlying idea of energy conversion is similar to other wave-based heating mechanisms: increasingly smaller length scales are created, until dissipation becomes important and converts kinetic and magnetic energy into heat. The main difference compared to other mechanisms is that in turbulence small scales are created nonlinearly (unlike in phase mixing, resonant absorption, etc.), producing an energy cascade to smaller scales (although, in some scenarios inverse cascade can also take place). We differentiate three main scales or ranges in turbulence, as depicted schematically in Fig. 10. The largest scale is the energy containing scale, at which the forcing of the plasma takes place, e.g. the size of convective cells in the photosphere (depicted in blue in Fig. 10). The inertial range is an intermediate scale where the actual energy cascade is initiated. The dynamics are self-similar and independent of both the nature of forcing and dissipation (shown in green in Fig. 10), expected to correspond to Kolmogorov power law indices of -5/3. Lastly, at scales where dissipative terms are on the order of advective terms (Reynolds and/or magnetic Reynolds numbers $\approx 1$), turbulence enters the dissipation range, where heat is generated (assuming collisional dissipation), displayed with the red zone in Fig. 10. In this last range, the power law index depends on the particular dissipation mechanism (e.g. electron or proton dissipation) that is considered, growing ever steeper.

The most researched turbulence-generating wave interaction is that of counter-propagating pure Alfvén waves in the incompressible limit. In this scenario, the Alfvén wave wavefronts are deformed in successive collisions, leading to a cascade towards higher wavenumbers (see Figure 11). In the corona, counter-propagating transverse or Alfvénic waves can exist in both closed structures, such as coronal loops, and open structures, due to wave reflection. Wave reflection occurs when the Alfvén speed varies along the propagation direction, i.e. along the background magnetic field, linearly coupling the outward and inward-propagating Alfvén waves (Leroy, 1980; Hollweg and Isenberg, 2007). Alfvén speed variations along the field exist in the corona because of gravitational stratification of the plasma, and the spherical/dipolar expansion of the magnetic field with height. In the turbulent heating models, the source of input energy is usually the convective flows in the photosphere, which generate waves and eventually turbulence by shuffling the magnetic field lines. There are numerous models of coronal heating based on turbulence for both coronal loops (van Ballegooijen et al., 2011; Downs et al., 2016; van Ballegooijen et al., 2017), and open structures (Perez and Chandran, 2013; Woolsey
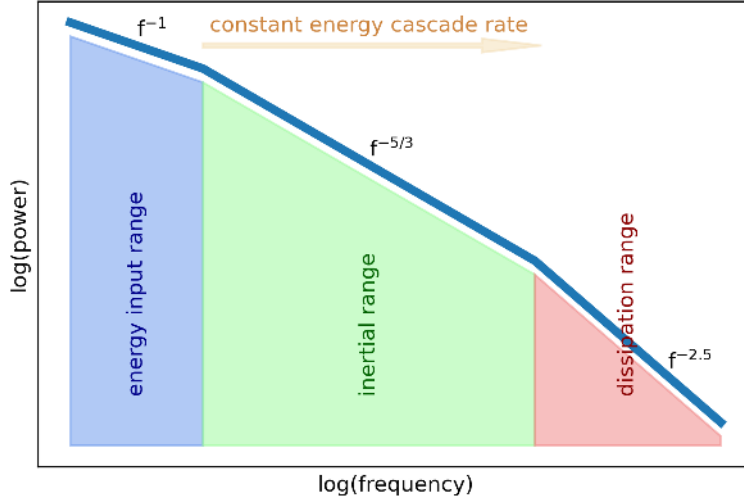
**Fig. 10** A schematic graph of the power law behaviour of turbulent fluctuations in the solar atmosphere and wind. The left, blue range shows the energy input range with a power law index of -1. The middle, green range shows the inertial range with a power law index of -5/3, where the energy cascade rate is independent of the scale. The right, red range shows the dissipation range, where the ever steeper power law slope depends on the specific dissipation process.

and Cranmer, 2015; Chandran and Perez, 2019), and also global models (van der Holst et al., 2014; Oran et al., 2017). The models for Alfvén wave heating of active regions (van Ballegooijen and Asgari-Targhi, 2018) show that temperatures reach maximally 2.5 MK, and that other heating mechanisms are needed to go beyond those temperatures.

The 'local' models mostly use a reduced MHD treatment, which neglects density perturbations (i.e., are incompressible) and transverse inhomogeneities in the plasma, among other simplifications. For the global models, Alfvén wave equations are employed in van der Holst et al. (2014), containing heavily approximated terms for reflection and turbulent dissipation, and Reynolds-averaged mean flow equations with turbulent transport in Usmanov et al. (2018). All these models conclude that a multi-million K corona can be maintained by turbulent heating, while balancing radiative cooling and conductive losses. A common discrepancy between turbulent heating models and observed properties of the corona is the excessive non-thermal line broadening that results from the models (Brooks and Warren, 2016).

Recently, it was realized that the existence of counterpropagating waves is not the only way to generate turbulence (Magyar et al., 2017, 2019). In the presence of transverse inhomogeneities, propagating Alfvénic waves can nonlinearly self-deform, generating a cascade to smaller scales, called uniturbulence (see Figure 12). This can constitute an additional channel towards a turbulent cascade and can
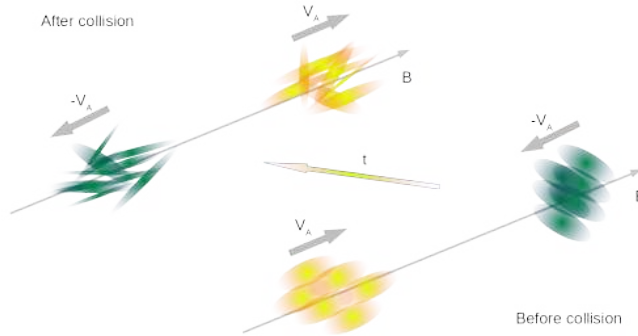
**Fig. 11** Illustrating the mutual deformation of two counter-propagating Alfvénic wave-packets along some background magnetic field **B**. The undisturbed wave-packets must collectively vary along both perpendicular directions for nonlinear interaction to occur (Howes and Nielson, 2013), depicted by the different orientation of the ellipsoid making up the packets. These ellipsoids can be considered isosurfaces of velocity perturbations. After the collision (on the upper left), the wave-packets are mutually deformed, leading to ellipsoids scattered to higher wavenumbers, i.e. appearing thinner.
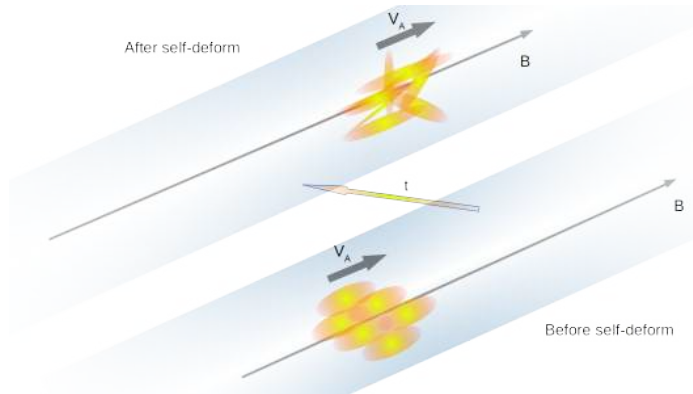


**Fig. 12** Same as in Figure 11, but having only the wave-packet propagating parallel to the magnetic field. The background plasma is inhomogeneous across the field. This is causing the initial Alfvénic wave-package to self-deform nonlinearly as it propagates, leading to elongated ellipsoids, i.e. cascading to higher wavenumbers.

potentially enhance the dissipation rate, leading to more heating. However, there are no models of coronal heating incorporating the effects of uniturbulence, as of yet. Still, forward modelling of simulations with uniturbulence (Pant et al., 2019) can elegantly and self-consistently explain the observed correlation between wave Doppler shift and spectral line broadening (McIntosh and De Pontieu, 2012, as also explained in Nakariakov et al.,2021).

Full 2.5D and 3D MHD models are now available (e.g. Dahlburg et al., 2012; Shoda et al., 2019) that take into account both the nonlinear Alfvén wave heating via compressive effects, and the Alfvén wave turbulence, and initial results seem to

point to the dominance of Alfvén wave turbulence over the compressive heating in the corona, while the opposite is true at the lower heights of the magnetic canopy (Matsumoto, 2016, 2018). Since these models target quiet Sun conditions for the loops it is not yet clear whether the same holds for the denser and more dynamic active region loop conditions.

To date, all Alfvén wave heating models have been mostly successful at generating and sustaining a lower energy budget corona as in the quiet Sun or coronal holes, while they all seem to fall short of the $10^4$ W m$^{-2}$ average heating rate needed for active region coronal loops (see chapter 6.1 Hinode Review Team et al., 2019, for a more thorough discussion). In particular, the hot loops at the core of active regions with temperatures of 5 MK or more seem to be unexplained by wave models in general (van Ballegooijen and Asgari-Targhi, 2018). Furthermore, these models seem to generate preferentially uniformly heated coronae in line with the RTV scaling law (Rosner et al., 1978), rather than footpoint heating. In turn, Alfvén wave heating models do not seem able to explain thermal non-equilibrium and the associated coronal rain (Antolin et al., 2010). Comparison of results from the Alfvén wave turbulence model with *Hinode*/EIS observations of active region loops indicates that longitudinal flows are an important ingredient, suggesting that either compressive effects may become important or that a different mechanism is present (Asgari-Targhi et al., 2014). It is important to note, however, that the very demanding computational requirements needed in fully consistent wave models strongly limit the current predictions (see section 4)

3.3 Kink-mode driven turbulent heating models

Standing transverse waves can be considered as superposition of counterpropagating waves, thus these can generate a turbulent cascade as well. In closed loops, initial perturbations such as flares, low coronal eruptions or shock waves can easily excite standing kink oscillations. Due to the shear motions between the loops and external corona, the Kelvin-Helmholtz instability can thus be induced near the loop boundary (Terradas et al., 2008a; Antolin et al., 2014, 2017; Magyar et al., 2015). Moreover, the generation of azimuthally polarised Alfvén waves due to resonant absorption increases the velocity shear with the external plasma, which can also enhance the instability (Antolin and Van Doorsselaere, 2019). The effect of the instability is to generate transverse wave induced Kelvin-Helmholtz rolls (TWIKH rolls), extended along the magnetic field, as shown in Fig. 13. The wave energy can dissipate efficiently if the turbulent structures are sufficiently developed. Direct comparison of such a model with observations of a prominence (Okamoto et al., 2015; Antolin et al., 2015), gives an indication that the emission is indeed shifting from a temperature of $10^4$ K to $10^5$ K after the passing of the transverse wave, in accordance with the numerical model (see Fig. 14). Recent studies by Antolin and Van Doorsselaere (2019) revealed that resonant absorption plays a key role in energizing and spreading the TWIKH rolls throughout a coronal loop.

The most basic setup that was used was a cylindrical loop with an initial velocity pulse, setting up a damped standing wave. This setup was used to show that the non-linearly developing KHI introduces an amplitude dependent damping (Magyar and Van Doorsselaere, 2016), which matches reasonably well with observations (Goddard et al., 2016a). As intuitively understood, the magnetic twist provides a
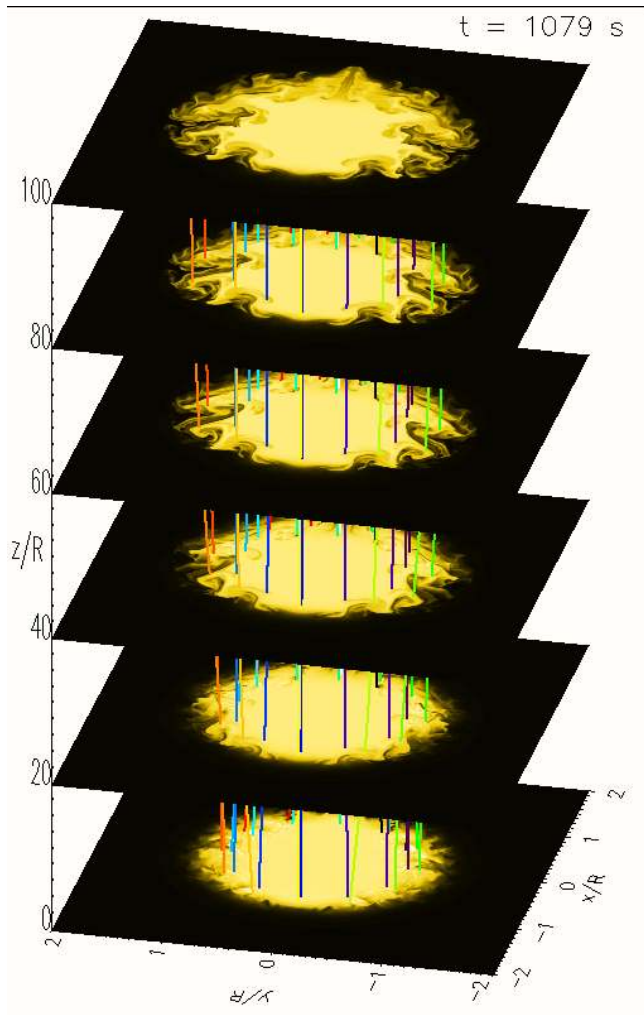
**Fig. 13** A tomography of TWIKH rolls. Cross-sections of density (in yellow) are shown at different locations along half the length of a prominence oscillating with a standing kink mode after roughly 2 periods. The coloured lines correspond to selected magnetic field lines traced from the bottom. The TWIKH rolls drag the field lines, generating twisting and strong changes in magnetic field pressure in a wide layer around the boundary. The simulation corresponds to the high resolution run discussed in Antolin et al. (2015).

stabilising effect (Howson et al., 2017a; Terradas et al., 2018), which delays the development of the instability without completely suppressing it. This corresponds well with the predictions from analytical models (Hillier et al., 2019; Barbulescu et al., 2019). Moreover, the stabilising effect of viscosity and resistivity was investigated numerically (Howson et al., 2017b; Karampelas et al., 2019a). However, as explained in Sec. 2.1, simple calculations using basic estimates show that the directly observed standing waves in the solar corona do not seem to contain sufficient energy for heating it.
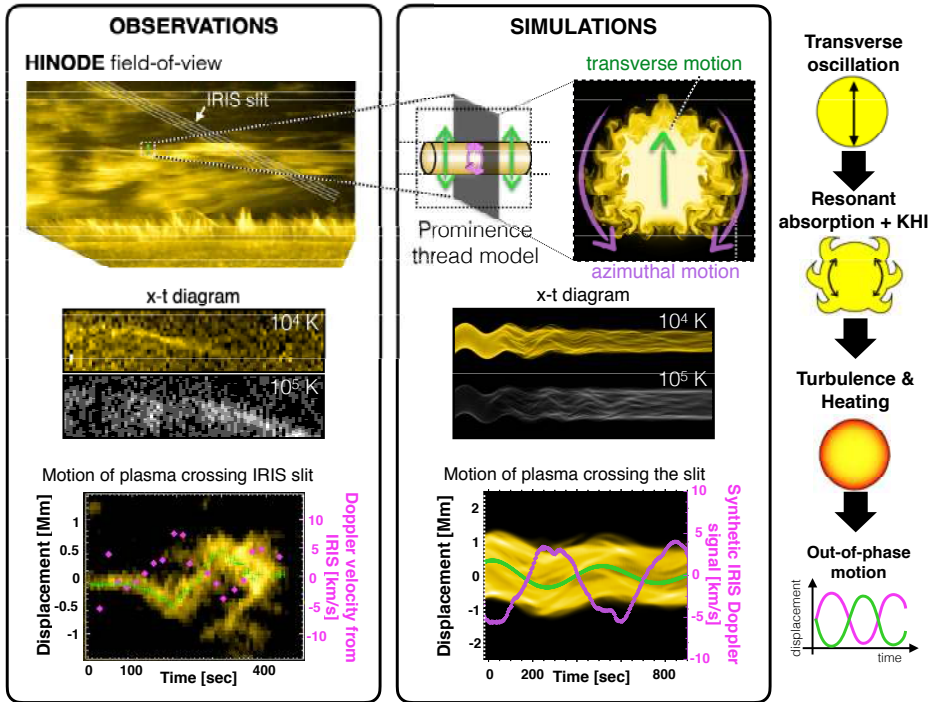
**Fig. 14** Evidence for resonant absorption and heating in a prominence. The left column provides a set of observables obtained with coordinated observations (top panel) between Hinode/SOT and IRIS of an active region prominence off-limb. (Left-middle) Prominence threads were seen oscillating transversely and fading in the Ca II H line of SOT ($10^4$ K) and subsequently appearing in the hotter SJI 1400 channel of IRIS (dominated by Si IV emission at $10^{4.8}$ K approximately). (Left-bottom) The prominence threads oscillate in the POS (yellow with green curve) out-of-phase with the Doppler velocity in Si IV captured by the IRIS slit (purple). The right column shows the forward modelling of a numerical simulation of a prominence thread with the observed characteristics. The thread oscillates transversely with a kink mode and triggers the KHI at the boundary (top-right). Resonant absorption is initially highly localised in the boundary, which fuels the KHI. TWIKH rolls are excited, whose dynamics reflect the resonant absorption and phase mixing dynamics but at a larger, observable scale. The TWIKH rolls mix the cold prominence plasma with the hot coronal surroundings and widen the boundary of the loop. A turbulent cascade is established which leads to wave dissipation and heating. As the prominence plasma is heated, its emission in the synthesised Ca II H line fades out and becomes stronger in the hotter Si IV line (right-middle). The resonant absorption and phase mixing dynamics become observable due to the KHI, leading to an out-of-phase relation between the POS motion of the thread and the Doppler velocity of the heated prominence plasma. A very good match is thus obtained with the observations. A sketch of the observed physical processes is given on the right. Adapted from Okamoto et al. (2015) and Antolin et al. (2015).

It was soon realised that the TWIKH rolls could play an important role if waves are driven at a loop footpoint. In that configuration, the TWIKH rolls provide an elegant mechanism to move the energy from the input scales, to the smaller length scales of the inertial range, and on to the dissipation scales at which the plasma is heated, just as Alfvén wave turbulence would do. This damping mechanism in the inertial range is independent of transport coefficients. In doing so, the energy

cascade balances the input energy, creating a (statistically) steady state, indirectly feeding the driving energy into plasma heating. The steady state that is obtained in the numerical models could be a potential model for the observed decayless observations.

In the setup with the footpoint driver in a closed loop, Karampelas and Van Doorsselaere (2018) obtained a fully deformed loop cross-section. Although the turbulence significantly changes the initial equilibrium, the loop structure can still be observed in forward models, meaning that turbulent loops probability exist in the real solar corona. Further studies (Karampelas et al., 2019a) considering gravity in a loop, stressed the importance of longitudinal stratification, which improves the efficiency of wave heating. The TWIKH roll formation dependence on the driver frequency was investigated by Afanasyev et al. (2019), who subsequently also considered the driving with a turbulent spectrum (Afanasyev et al., 2020).

Considering the turbulent motions at the footpoint of a coronal loop anchored in the photosphere, Guo et al. (2019b) employed a mixed transverse and torsional driver at the loop footpoint, going beyond the implicitly excited Alfvén waves in the simulations of Pascoe et al. (2011). Comparing with a pure kink driven loop and a pure torsional driven loop, they found that the KHI eddies are fully developed in the whole loop cross-section and that internal energy and temperature in the mixed driven loop are higher. This means that the mixed modes lead to a more efficient dissipation in the turbulent state of plasma and that the KHI acts as an agent to dissipate energy in both wave modes. In addition, forward models showed very similar images to the observations of decayless oscillations. This means that the ubiquitous decayless oscillations could play an important role in coronal heating. However, as is shown in Figure 15, due to the limited resolution of instruments, neither Alfvén modes nor the fine structures are observable. This means that although difficult to capture, Alfvén modes probably can coexist with kink modes, leading to enhanced heating.

A further study by Guo et al. (2019a) examined how such a mixed mode driver affects a tightly packed multi-stranded loop. By depositing almost identical input energy flux at the footpoint of a multi-stranded loop and a density equivalent monolithic loop, Guo et al. (2019a) found that the multi-stranded loop is more efficient in starting the heating process due to the quickly established turbulent state in this model.

Again using a model with footpoint driven loops, Karampelas et al. (2019b) computed the dependence of the wave amplitude as they would be observed from forward modelling, on the driver amplitude. They found that there is only a weak dependence between both. Thus, they showed that the amplitude of the decayless waves is actually an unrealiable measure of the wave energy that is being dissipated in the solar corona, as studied in more detail by Hillier et al. (2020). Karampelas et al. (2019b) concluded that the spectral line broadening is a much more accurate quantity to give a measure of the wave energy that is being dissipated. This may influence assessments of energy content and flux of standing or propagating kink waves (as e.g. in Sec. 2.1).

Even though these models seem promising, at the time of submission, there is no published paper in which the non-linearly evolving, footpoint-driven transverse waves can compensate the radiative or thermal conduction cooling of the coronal plasma in a self-consistent model, contrary to DC heating models of the solar corona (e.g. Hansteen et al., 2015). But, it should be noted that the 3D MHD DC
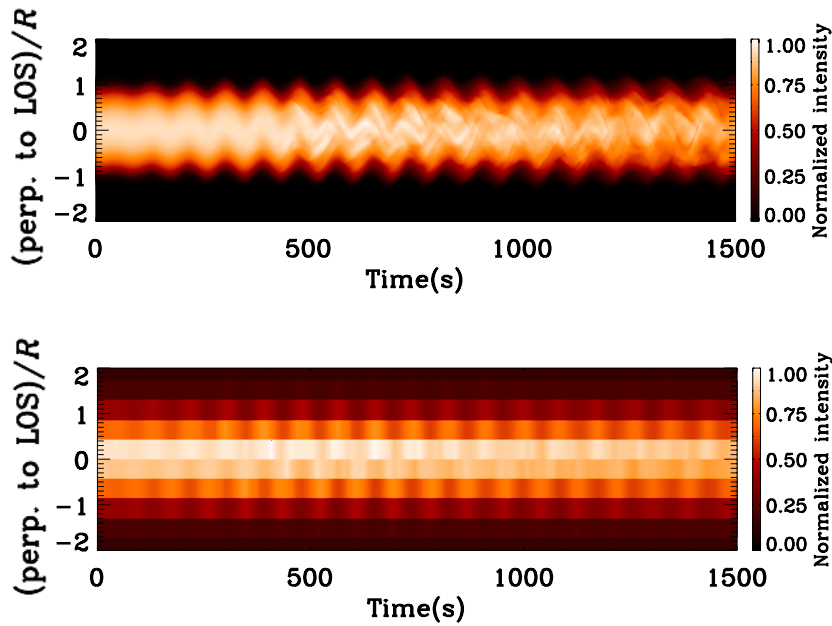
**Fig. 15** Forward-modelling results for the numerical models in the Fe IX 171 $\mathring{A}$ line at the apex with an LOS angle of 45°. The upper row is obtained with the full numerical resolution and the lower row with a degraded resolution comparable to SDO/AIA. Figure taken from Guo et al. (2019b).

models usually employ unrealistically high resistivity and viscosity, which are the sources for the heating in them.

## 4 Critical Assessment & Conclusions

This review provides an overview of the progress made in (roughly) the last decade in observations and models of wave heating in the solar corona. A lot of progress has been made in wave-based heating mechanisms using a combination of advanced high-resolution satellite and ground-based solar observations, and advances in computational MHD modeling.

From an observational point of view, we now have detailed observations of several wave modes that could play a role in heating the corona. Recent multi-wavelength studies of coronal loops have not found evidence of any significant heating following large-amplitude kink oscillations (Goddard and Nisticò, 2020; Pascoe et al., 2020). However, decayless kink oscillations and quasi-periodic propagating fast waves could potentially account for coronal losses in certain regions. We now have several observational characterisations of the wave energy content in the solar corona, based on imaging, spectroscopy or spectropolarimetry. In the chromosphere, a very large energy flux is found in waves, and if even only a fraction of that is dissipated in the corona, it is heated efficiently. In the corona itself, wave observations find energy fluxes comparable to the required heating rate, but also one or two orders of magnitude below it, particularly in the case of active regions.

This wide disparity in observational estimates of coronal wave energy points to a variety of wave activity manifestations, and probably indicates that the issue of coronal wave energy requires further study. The latter point is also underlined by the discrepancy between the energy flux in numerical models and their forward modelling (De Moortel and Pascoe, 2012; Van Doorsselaere et al., 2014; Karampelas et al., 2019b).

From the modelling point of view, the computational models have been lifted to a new level in recent years thanks to advancement in computational power. Now, 3D MHD simulations are the norm. In addition to previously considered AC heating mechanisms by non-linear Alfvén waves, these 3D MHD simulations show that turbulence and development of small scales is important. Simulations of Alfvén wave turbulence in (perpendicularly) uniform plasmas are able to maintain coronal temperatures, even in 3D configurations. In order to take into account the perpendicular density structuring, studies have focused on phase mixing and the transverse wave induced Kelvin-Helmholtz instability. Despite the strong effort in these last two subjects, still no self-consistent simulation exists in which a density enhanced coronal loop is maintained against cooling by radiation or conduction, with resolved wave energy flux from the photosphere.

Self-consistent wave modelling studies are extremely demanding in computational power. The photospheric source (or sub-photopheric), the chromosphere (rich in wave processes due to its high- to low-$\beta$ variable conditions), the transition region (in which the Alfvén speed steepens leading to reflection, refraction and mode conversion) and the corona (in which small density inhomogeneities and wave-to-wave interaction are important) need to be included in the model. In addition, the resolution needs to be high enough to allow wave-associated instabilities and the turbulent spectrum to set in with the inertial range established for at least a decade in wave number. Through the decades, these limitations have favoured the investigation of wave dissipation in waveguides that are already well-defined (such as coronal loops) without the connection to other atmospheric layers (the latter is only recently changing, e.g. Van Damme et al., 2020). Although limiting, this approach has lead to an essential categorisation of wave processes and wave dissipation locally, and to phase relations between observables for a direct comparison with high resolution observations (Hinode Review Team et al., 2019, chapter 6.1). It remains to be seen how these models connect to more advanced models of wave propagation in the lower atmosphere (e.g. Felipe et al., 2011).

This approach has also allowed to investigate the relative importance of specific wave mechanisms and the available energy at the coronal base (e.g. Soler et al., 2019). Improvements in numerical techniques and increased computation power are coming close to allowing self-consistent modelling which incorporates all the relevant wave processes in a large scale model (such as a whole active region). This would allow to fully account for nonlinear processes and, in particular, global observables of wave heating models for an easier comparison with observations.

These recent developments have made it clear that the omnipresent coronal waves also strongly influence DC heating models.
Firstly, due to the observed continuous influx of Alfvénic waves into the corona, it is expected that the resulting heating is more continuous and less impulsive than that obtained from magnetic reconnection alone. This long-standing assumption is only true if waves and reconnection act in a sufficiently independent way from each other. However, we can think of scenarios in which one facilitates the other. For

instance, reconnection-based nanoflares in the corona are based on the braiding scenario, through which the magnetic field is stressed to a certain degree before releasing these stresses through component (small-angle) reconnection, thus leading to impulsive, middle to low-frequency events (see chapter 6.2 in Hinode Review Team et al., 2019). Moreover, transverse wave induced Kelvin-Helmholtz rolls (see Sec. 3.3) create local twists and small-angle misalignments between the strands and, as in the magnetopause (Nykyri and Otto, 2004), magnetic reconnection is expected. In this scenario, the heating from reconnection is expected to be impulsive and act only when the KHI is triggered. Although twists delay the formation of the KHI, they do not inhibit the instability (see Sec. 3.3). Further investigation of this scenario is therefore needed.

Secondly, DC heating models are often based on stranded loop models, in which each magnetic field line is modelled independently from each other (Reale, 2014). The turbulence appearing in Alfvén wave and kink wave models of loops are very efficient at mixing plasma perpendicular to the magnetic field (Magyar and Van Doorsselaere, 2016). This mixing induces adiabatic expansion and contraction of plasma elements, leading to (apparent) cooling and heating on particular field lines, which is not taken into account if they are completely decoupled. Moreover, additional magnetic pressure enhancements are introduced, leading to a restructuring of the plasma in the single fieldline models.

Thirdly, the nonlinearly induced perturbations due to Alfvén waves are not restricted to funnels and flux tubes with transverse or parallel structuring, but also feature in magnetic reconnection sites when Alfvén waves interact with a magnetic null point. As the Alfvén wave nears the magnetic null-point it induces magnetoacoustic waves which in turn contribute towards heating at the null point (Galsgaard et al., 2003; Thurgood and McLaughlin, 2013; Sabri et al., 2018). The fast and slow magnetoacoustic waves experience shocks in the vicinity of the null-point leading to enhanced dissipation there (McLaughlin et al., 2009; Sabri et al., 2018). Thus, despite the Alfvén wave being unable to reach the null point while travelling along the separatrices, their coupling to the magnetoacoustic waves provides an agent to their gradual dissipation and contribution towards heating near X-points (McLaughlin and Hood, 2004, 2006).

Overall, we conclude this review with the following one-liner: Motivated by plentiful recent observations of coronal waves, AC heating models have taken a leap forward in recent years, but have not yet managed to self-consistently maintain loops at the observed million degree temperatures. These models make it worthwhile to have a renewed look at DC heating models while including the cross-field effects induced by wave dynamics.

# References

Afanasyev A, Karampelas K, Van Doorsselaere T (2019) Coronal Loop Transverse Oscillations Excited by Different Driver Frequencies. ApJ876(2):100, DOI 10.3847/1538-4357/ab1848, 1905.05716

Afanasyev AN, Van Doorsselaere T, Nakariakov VM (2020) Excitation of decayless transverse oscillations of coronal loops by random motions. A&A633:L8, DOI 10.1051/0004-6361/201937187, 1912.07980

Alfvén H (1947) Magneto hydrodynamic waves, and the heating of the solar corona. MNRAS107:211, DOI 10.1093/mnras/107.2.211

Anfinogentov SA, Nakariakov VM (2019) Magnetohydrodynamic Seismology of Quiet Solar Active Regions. ApJ884(2):L40, DOI 10.3847/2041-8213/ab4792, 1910.03809

Anfinogentov SA, Nakariakov VM, Nisticò G (2015) Decayless low-amplitude kink oscillations: a common phenomenon in the solar corona? A&A583:A136, DOI 10.1051/0004-6361/201526195, 1509.05519

Antolin P, Shibata K (2010) The Role Of Torsional Alfvén Waves in Coronal Heating. ApJ712(1):494–510, DOI 10.1088/0004-637X/712/1/494, 0910.0962

Antolin P, Van Doorsselaere T (2019) Influence of resonant absorption on the generation of the Kelvin-Helmholtz Instability. Frontiers in Physics 7:85, DOI 10.3389/fphy.2019.00085

Antolin P, Verwichte E (2011) Transverse Oscillations of Loops with Coronal Rain Observed by Hinode/Solar Optical Telescope. ApJ736:121–+, DOI 10.1088/0004-637X/736/2/121, 1105.2175

Antolin P, Shibata K, Kudoh T, Shiota D, Brooks D (2008) Predicting Observational Signatures of Coronal Heating by Alfvén Waves and Nanoflares. ApJ688:669-682, DOI 10.1086/591998

Antolin P, Shibata K, Vissers G (2010) Coronal Rain as a Marker for Coronal Heating Mechanisms. ApJ716:154–166, DOI 10.1088/0004-637X/716/1/154, 0910.2383

Antolin P, Yokoyama T, Van Doorsselaere T (2014) Fine Strand-like Structure in the Solar Corona from Magnetohydrodynamic Transverse Oscillations. ApJ787:L22, DOI 10.1088/2041-8205/787/2/L22, 1405.0076

Antolin P, Okamoto TJ, De Pontieu B, Uitenbroek H, Van Doorsselaere T, Yokoyama T (2015) Resonant Absorption of Transverse Oscillations and As-

sociated Heating in a Solar Prominence. II. Numerical Aspects. ApJ809:72,
    DOI 10.1088/0004-637X/809/1/72, 1506.09108

Antolin P, De Moortel I, Van Doorsselaere T, Yokoyama T (2016) Modeling
    Observed Decay-less Oscillations as Resonantly Enhanced Kelvin-Helmholtz
    Vortices from Transverse MHD Waves and Their Seismological Application.
    ApJ830:L22, DOI 10.3847/2041-8205/830/2/L22, 1609.09716

Antolin P, De Moortel I, Van Doorsselaere T, Yokoyama T (2017) Obser-
    vational Signatures of Transverse Magnetohydrodynamic Waves and Associ-
    ated Dynamic Instabilities in Coronal Flux Tubes. ApJ836:219, DOI 10.3847/
    1538-4357/aa5eb2

Antolin P, Pagano P, De Moortel I, Nakariakov VM (2018a) In Situ Generation
    of Transverse Magnetohydrodynamic Waves from Colliding Flows in the Solar
    Corona. ApJ861:L15, DOI 10.3847/2041-8213/aacf98, 1807.00395

Antolin P, Schmit D, Pereira TMD, De Pontieu B, De Moortel I (2018b) Transverse
    Wave Induced Kelvin-Helmholtz Rolls in Spicules. ApJ856(1):44, DOI 10.3847/
    1538-4357/aab34f, 1803.00821

Arber TD, Brady CS, Shelyag S (2016) Alfvén Wave Heating of the Solar
    Chromosphere: 1.5D Models. ApJ817(2):94, DOI 10.3847/0004-637X/817/2/94,
    1512.05816

Arregui I (2015) Wave heating of the solar atmosphere. Philosophical Transactions
    of the Royal Society of London Series A 373(2042):20140261–20140261, DOI
    10.1098/rsta.2014.0261, 1501.06708

Arregui I, Soler R, Ballester JL, Wright AN (2011) Magnetohydrodynamic kink
    waves in two-dimensional non-uniform prominence threads. A&A533:A60, DOI
    10.1051/0004-6361/201117477, 1011.5175

Aschwanden MJ (2004) Physics of the Solar Corona. An Introduction. Praxis
    Publishing Ltd., Chichester, UK, and Springer-Verlag Berlin

Aschwanden MJ (2019) New Millennium Solar Physics, vol 458. DOI 10.1007/
    978-3-030-13956-8

Aschwanden MJ, Fletcher L, Schrijver CJ, Alexander D (1999) Coronal Loop Oscil-
    lations Observed with the Transition Region and Coronal Explorer. ApJ520:880–
    894

Asgari-Targhi M, van Ballegooijen AA, Imada S (2014) Comparison of Extreme
    Ultraviolet Imaging Spectrometer Observations of Solar Coronal Loops with
    Alfvén Wave Turbulence Models. ApJ786(1):28, DOI 10.1088/0004-637X/786/
    1/28

Bale SD, Badman ST, Bonnell JW, Bowen TA, Burgess D, Case AW, Cattell CA,
    Chandran BDG, Chaston CC, Chen CHK, Drake JF, de Wit TD, Eastwood
    JP, Ergun RE, Farrell WM, Fong C, Goetz K, Goldstein M, Goodrich KA,
    Harvey PR, Horbury TS, Howes GG, Kasper JC, Kellogg PJ, Klimchuk JA,
    Korreck KE, Krasnoselskikh VV, Krucker S, Laker R, Larson DE, MacDowall
    RJ, Maksimovic M, Malaspina DM, Martinez-Oliveros J, McComas DJ, Meyer-
    Vernet N, Moncuquet M, Mozer FS, Phan TD, Pulupa M, Raouafi NE, Salem
    C, Stansby D, Stevens M, Szabo A, Velli M, Woolley T, Wygant JR (2019)
    Highly structured slow solar wind emerging from an equatorial coronal hole.
    Nature576(7786):237–242, DOI 10.1038/s41586-019-1818-7

Banerjee D, Teriaca L, Doyle JG, Wilhelm K (1998) Broadening of SI VIII lines
    observed in the solar polar coronal holes. A&A339:208–214

Barbulescu M, Ruderman MS, Van Doorsselaere T, Erdélyi R (2019) An Ana-

lytical Model of the Kelvin-Helmholtz Instability of Transverse Coronal Loop Oscillations. ApJ870(2):108, DOI 10.3847/1538-4357/aaf506, 1901.06132

Belien AJC, Poedts S, Spoelder HJW, Leenders R, Goedbloed JP (1996) Visualization of resonant absorption in solar coronal loops by simulation of soft X-ray images. Computers in Physics 10(6):573–583, DOI 10.1063/1.168586

Berghmans D, Clette F (1999) Active region euv transient brightenings – first results by eit of soho jop80. Sol. Phys.186:207–229, DOI 10.1023/A:1005189508371

Brady CS, Arber TD (2016) Simulations of Alfvén and Kink Wave Driving of the Solar Chromosphere: Efficient Heating and Spicule Launching. ApJ829(2):80, DOI 10.3847/0004-637X/829/2/80, 1601.07835

Brooks DH, Warren HP (2016) Measurements of Non-thermal Line Widths in Solar Active Regions. ApJ820(1):63, DOI 10.3847/0004-637X/820/1/63, 1511.02313

Bruno R, Carbone V (2013) The Solar Wind as a Turbulence Laboratory. Living Reviews in Solar Physics 10(1):2, DOI 10.12942/lrsp-2013-2

Cally PS (2017) Alfvén waves in the structured solar corona. MNRAS466(1):413–424, DOI 10.1093/mnras/stw3215, 1612.02064

Cally PS, Hansen SC (2011) Benchmarking Fast-to-Alfvén Mode Conversion in a Cold Magnetohydrodynamic Plasma. ApJ738:119, DOI 10.1088/0004-637X/738/2/119, 1105.5754

Cargill PJ, De Moortel I, Kiddie G (2016) Coronal Density Structure and its Role in Wave Damping in Loops. ApJ823(1):31, DOI 10.3847/0004-637X/823/1/31

Carlqvist P (1979) A flare-associated mechanism for solar surges. Sol. Phys.63(2):353–367, DOI 10.1007/BF00174540

Chae J, Schühle U, Lemaire P (1998) SUMER Measurements of Nonthermal Motions: Constraints on Coronal Heating Mechanisms. ApJ505:957–973, DOI 10.1086/306179

Chandran BDG, Perez JC (2019) Reflection-driven magnetohydrodynamic turbulence in the solar atmosphere and solar wind. Journal of Plasma Physics 85(4):905850409, DOI 10.1017/S0022377819000540, 1908.00880

Chen L, Hasegawa A (1974) A theory of long-period magnetic pulsations: 1. steady state excitation of field line resonance. Journal of Geophysical Research 79(7):1024–1032, DOI 10.1029/JA079i007p01024, URL http://dx.doi.org/10.1029/JA079i007p01024

Claes N, Keppens R (2019) Thermal stability of magnetohydrodynamic modes in homogeneous plasmas. A&A624:A96, DOI 10.1051/0004-6361/201834699

Copil P, Voitenko Y, Goossens M (2008) Torsional Alfvén waves in small scale density threads of the solar corona. A&A478(3):921–927, DOI 10.1051/0004-6361:20078481

Cowling TG (1953) Solar Electrodynamics, p 532

Cranmer SR, van Ballegooijen AA (2005) On the Generation, Propagation, and Reflection of Alfvén Waves from the Solar Photosphere to the Distant Heliosphere. ApJS156(2):265–293, DOI 10.1086/426507, astro-ph/0410639

Culhane JL, Harra LK, James AM, Al-Janabi K, Bradley LJ, Chaudry RA, Rees K, Tandy JA, Thomas P, Whillock MCR, Winter B, Doschek GA, Korendyke CM, Brown CM, Myers S, Mariska J, Seely J, Lang J, Kent BJ, Shaughnessy BM, Young PR, Simnett GM, Castelli CM, Mahmoud S, Mapson-Menard H, Probyn BJ, Thomas RJ, Davila J, Dere K, Windt D, Shea J, Hagood R, Moye R, Hara H, Watanabe T, Matsuzaki K, Kosugi T, Hansteen V, Wikstol Ø (2007) The EUV Imaging Spectrometer for Hinode. Sol. Phys.243:19–61, DOI 10.1007/

s01007-007-0293-1

Dahlburg RB, Einaudi G, Rappazzo AF, Velli M (2012) Turbulent coronal heating mechanisms: coupling of dynamics and thermodynamics. A&A544:L20, DOI 10.1051/0004-6361/201219752, 1208.2459

De Moortel I, Nakariakov VM (2012) Magnetohydrodynamic waves and coronal seismology: an overview of recent results. Royal Society of London Philosophical Transactions Series A 370:3193–3216, DOI 10.1098/rsta.2011.0640, 1202.1944

De Moortel I, Pascoe DJ (2012) The Effects of Line-of-sight Integration on Multi-strand Coronal Loop Oscillations. ApJ746:31, DOI 10.1088/0004-637X/746/1/31

De Pontieu B, Martens PCH, Hudson HS (2001) Chromospheric Damping of Alfvén Waves. ApJ558:859–871

De Pontieu B, McIntosh SW, Carlsson M, Hansteen VH, Tarbell TD, Schrijver CJ, Title AM, Shine RA, Tsuneta S, Katsukawa Y, Ichimoto K, Suematsu Y, Shimizu T, Nagata S (2007) Chromospheric Alfvénic Waves Strong Enough to Power the Solar Wind. Science 318:1574–, DOI 10.1126/science.1151747

De Pontieu B, Carlsson M, Rouppe van der Voort LHM, Rutten RJ, Hansteen VH, Watanabe H (2012) Ubiquitous Torsional Motions in Type II Spicules. ApJ752:L12, DOI 10.1088/2041-8205/752/1/L12, 1205.5006

Dere KP, Mason HE (1993) Nonthermal velocities in the solar transition zone observed with the high-resolution telescope and spectrograph. Sol. Phys.144:217–241, DOI 10.1007/BF00627590

Dere KP, Landi E, Mason HE, Monsignori Fossi BC, Young PR (1997) CHIANTI - an atomic database for emission lines. A&AS125:149–173, DOI 10.1051/aas:1997368

Dere KP, Del Zanna G, Young PR, Landi E, Sutherland RS (2019) CHIANTI—An Atomic Database for Emission Lines. XV. Version 9, Improvements for the X-Ray Satellite Lines. ApJS241(2):22, DOI 10.3847/1538-4365/ab05cf, 1902.05019

Downs C, Lionello R, Mikić Z, Linker JA, Velli M (2016) Closed-field Coronal Heating Driven by Wave Turbulence. ApJ832(2):180, DOI 10.3847/0004-637X/832/2/180, 1610.02113

Edwin PM, Roberts B (1983) Wave propagation in a magnetic cylinder. Sol. Phys.88:179–191

Evans RM, Opher M, Jatenco-Pereira V, Gombosi TI (2009) Surface Alfvén Wave Damping in a Three-Dimensional Simulation of the Solar Wind. ApJ703(1):179–186, DOI 10.1088/0004-637X/703/1/179, 0908.3146

Feldman U, Doschek GA, Seely JF (1988) Solar spectroscopy in the far-ultraviolet-X-ray wavelength regions - Status and prospects. Journal of the Optical Society of America B Optical Physics 5:2237–2251, DOI 10.1364/JOSAB.5.002237

Felipe T (2012) Three-dimensional Numerical Simulations of Fast-to-Alfvén Conversion in Sunspots. ApJ758(2):96, DOI 10.1088/0004-637X/758/2/96, 1208.5726

Felipe T, Khomenko E, Collados M (2011) Magnetoacoustic Wave Energy from Numerical Simulations of an Observed Sunspot Umbra. ApJ735(1):65, DOI 10.1088/0004-637X/735/1/65, 1104.4138

Field GB (1965) Thermal Instability. ApJ142:531, DOI 10.1086/148317

Fujimura D, Tsuneta S (2009) Properties of Magnetohydrodynamic Waves in the Solar Photosphere Obtained with Hinode. ApJ702:1443–1457, DOI 10.1088/0004-637X/702/2/1443, 0907.3025

Galsgaard K, Priest ER, Titov VS (2003) Numerical experiments on wave propagation towards a 3D null point due to rotational motions. Journal of Geophysical Research (Space Physics) 108(A1):1042, DOI 10.1029/2002JA009393

Goddard CR, Nisticò G (2020) Temporal evolution of oscillating coronal loops. A&A638:A89, DOI 10.1051/0004-6361/202037467, `2004.14725`

Goddard CR, Nisticò G, Nakariakov VM, Zimovets IV (2016a) A statistical study of decaying kink oscillations detected using SDO/AIA. A&A585:A137, DOI 10.1051/0004-6361/201527341, `1511.03558`

Goddard CR, Nisticò G, Nakariakov VM, Zimovets IV, White SM (2016b) Observation of quasi-periodic solar radio bursts associated with propagating fast-mode waves. A&A594:A96, DOI 10.1051/0004-6361/201628478, `1608.04232`

Goedbloed JP, Poedts S (2004) Principles of magnetohydrodynamics. Cambridge University Press

Goossens M, Terradas J, Andries J, Arregui I, Ballester JL (2009) On the nature of kink MHD waves in magnetic flux tubes. A&A503:213–223, DOI 10.1051/0004-6361/200912399, `0905.0425`

Goossens M, Erdélyi R, Ruderman MS (2011) Resonant MHD Waves in the Solar Atmosphere. Space Sci. Rev.158:289–338, DOI 10.1007/s11214-010-9702-7

Goossens M, Andries J, Soler R, Van Doorsselaere T, Arregui I, Terradas J (2012) Surface Alfvén Waves in Solar Flux Tubes. ApJ753:111, DOI 10.1088/0004-637X/753/2/111, `1205.0935`

Goossens M, Van Doorsselaere T, Soler R, Verth G (2013) Energy Content and Propagation in Transverse Solar Atmospheric Waves. ApJ768:191, DOI 10.1088/0004-637X/768/2/191

Grant SDT, Jess DB, Moreels MG, Morton RJ, Christian DJ, Giagkiozis I, Verth G, Fedun V, Keys PH, Van Doorsselaere T, Erdélyi R (2015) Wave Damping Observed in Upwardly Propagating Sausage-mode Oscillations Contained within a Magnetic Pore. ApJ806(1):132, DOI 10.1088/0004-637X/806/1/132, `1505.01484`

Grant SDT, Jess DB, Zaqarashvili TV, Beck C, Socas-Navarro H, Aschwanden MJ, Keys PH, Christian DJ, Houston SJ, Hewitt RL (2018) Alfvén wave dissipation in the solar chromosphere. Nature Physics 14(5):480–483, DOI 10.1038/s41567-018-0058-3, `1810.07712`

Gudiksen BV, Nordlund Å (2005) An Ab Initio Approach to the Solar Coronal Heating Problem. ApJ618:1020–1030, DOI 10.1086/426063, `astro-ph/0407266`

Guo M, Van Doorsselaere T, Karampelas K, Li B (2019a) Wave Heating in Simulated Multistranded Coronal Loops. ApJ883(1):20, DOI 10.3847/1538-4357/ab338e, `1907.08013`

Guo M, Van Doorsselaere T, Karampelas K, Li B, Antolin P, De Moortel I (2019b) Heating Effects from Driven Transverse and Alfvén Waves in Coronal Loops. ApJ870(2):55, DOI 10.3847/1538-4357/aaf1d0, `1811.07608`

Hahn M, Savin DW (2013) Observational Quantification of the Energy Dissipated by Alfvén Waves in a Polar Coronal Hole: Evidence that Waves Drive the Fast Solar Wind. ApJ776(2):78, DOI 10.1088/0004-637X/776/2/78, `1302.5403`

Hahn M, Savin DW (2014) Evidence for Wave Heating of the Quiet-Sun Corona. ApJ795(2):111, DOI 10.1088/0004-637X/795/2/111, `1407.3250`

Hansteen V, Guerreiro N, De Pontieu B, Carlsson M (2015) Numerical Simulations of Coronal Heating through Footpoint Braiding. ApJ811(2):106, DOI 10.1088/0004-637X/811/2/106, `1508.07234`

Heyvaerts J, Priest ER (1983) Coronal heating by phase-mixed shear Alfven waves. A&A117:220–234

Hillier A, Barker A, Arregui I, Latter H (2019) On Kelvin-Helmholtz and parametric instabilities driven by coronal waves. MNRAS482(1):1143–1153, DOI 10.1093/mnras/sty2742, 1810.02773

Hillier A, Van Doorsselaere T, Karampelas K (2020) Estimating the Energy Dissipation from Kelvin-Helmholtz Instability Induced Turbulence in Oscillating Coronal Loops. ApJ897(1):L13, DOI 10.3847/2041-8213/ab9ca3, 2007.09068

Hinode Review Team, Al-Janabi, Khalid, Antolin, Patrick, Baker, Deborah, Bellot Rubio, Luis R, Bradley, Louisa, Brooks, David H, Centeno, Rebecca, Culhane, J Leonard, Del Zanna, Giulio, Doschek, George A, Fletcher, Lyndsay, Hara, Hirohisa, Harra, Louise K, Hillier, Andrew S, Imada, Shinsuke, Klimchuk, James A, Mariska, John T, Pereira, Tiago M D, Reeves, Katharine K, Sakao, Taro, Sakurai, Takashi, Shimizu, Toshifumi, Shimojo, Masumi, Shiota, Daikou, Solanki, Sami K, Sterling, Alphonse C, Su, Yingna, Suematsu, Yoshinori, Tarbell, Theodore D, Tiwari, Sanjiv K, Toriumi, Shin, Ugarte-Urra, Ignacio, Warren, Harry P, Watanabe, Tetsuya, Young, Peter R (2019) Achievements of Hinode in the first eleven years. Publications of the Astronomical Society of Japan 71(5), DOI 10.1093/pasj/psz084, URL https://doi.org/10.1093/pasj/psz084, r1, http://oup.prod.sis.lan/pasj/article-pdf/71/5/R1/30161340/psz084.pdf

Hollweg JV (1984) Resonances of coronal loops. ApJ277:392 – 403

Hollweg JV (1990) On WKB expansions for Alfven waves in the solar wind. J. Geophys. Res.95:14873–14879, DOI 10.1029/JA095iA09p14873

Hollweg JV, Isenberg PA (2007) Reflection of Alfvén waves in the corona and solar wind: An impulse function approach. Journal of Geophysical Research (Space Physics) 112:A08102, DOI 10.1029/2007JA012253

Hollweg JV, Jackson S, Galloway D (1982) Alfven waves in the solar atmosphere. III - Nonlinear waves on open flux tubes. Sol. Phys.75:35–61, DOI 10.1007/BF00153458

Howes GG, Nielson KD (2013) Alfvén wave collisions, the fundamental building block of plasma turbulence. I. Asymptotic solution. Physics of Plasmas 20(7):072302, DOI 10.1063/1.4812805, 1306.1455

Howson TA, De Moortel I, Antolin P (2017a) Energetics of the Kelvin-Helmholtz instability induced by transverse waves in twisted coronal loops. A&A607:A77, DOI 10.1051/0004-6361/201731178, 1708.04124

Howson TA, De Moortel I, Antolin P (2017b) The effects of resistivity and viscosity on the Kelvin- Helmholtz instability in oscillating coronal loops. A&A602:A74, DOI 10.1051/0004-6361/201630259, 1703.02423

Ionson JA (1978) ApJ226:650 – 673

Jenkins A (2013) Self-oscillation. Phys. Rep.525(2):167–222, DOI 10.1016/j.physrep.2012.10.007, 1109.6640

Jess DB, Mathioudakis M, Erdélyi R, Crockett PJ, Keenan FP, Christian DJ (2009) Alfvén Waves in the Lower Solar Atmosphere. Science 323(5921):1582, DOI 10.1126/science.1168680, 0903.3546

Jess DB, Van Doorsselaere T, Verth G, Fedun V, Krishna Prasad S, Erdélyi R, Keys PH, Grant SDT, Uitenbroek H, Christian DJ (2017) An Inside Look at Sunspot Oscillations with Higher Azimuthal Wavenumbers. ApJ842(1):59, DOI 10.3847/1538-4357/aa73d6, 1705.06282

Jess DB, Snow B, Houston SJ, Botha GJJ, Fleck B, Krishna Prasad S, Asensio
    Ramos A, Morton RJ, Keys PH, Jafarzadeh S, Stangalini M, Grant SDT, Chris-
    tian DJ (2019) A chromospheric resonance cavity in a sunspot mapped with
    seismology. Nature Astronomy 4:220–227, DOI 10.1038/s41550-019-0945-2

Karampelas K, Van Doorsselaere T (2018) Simulations of fully deformed oscillating
    flux tubes. A&A610:L9, DOI 10.1051/0004-6361/201731646, 1801.07657

Karampelas K, Van Doorsselaere T, Antolin P (2017) Heating by transverse waves
    in simulated coronal loops. A&A604:A130, DOI 10.1051/0004-6361/201730598,
    1706.02640

Karampelas K, Van Doorsselaere T, Guo M (2019a) Wave heating in gravita-
    tionally stratified coronal loops in the presence of resistivity and viscosity.
    A&A623:A53, DOI 10.1051/0004-6361/201834309, 1901.02676

Karampelas K, Van Doorsselaere T, Pascoe DJ, Guo M, Antolin P (2019b) Am-
    plitudes and energy fluxes of simulated decayless kink oscillations. Frontiers in
    Astronomy and Space Sciences 6:38, DOI 10.3389/fspas.2019.00038, 1906.02001

Keys PH, Morton RJ, Jess DB, Verth G, Grant SDT, Mathioudakis M, Mackay
    DH, Doyle JG, Christian DJ, Keenan FP, Erdélyi R (2018) Photospheric Ob-
    servations of Surface and Body Modes in Solar Magnetic Pores. ApJ857(1):28,
    DOI 10.3847/1538-4357/aab432, 1803.01859

Kitagawa N, Yokoyama T, Imada S, Hara H (2010) Mode Identification of MHD
    Waves in an Active Region Observed with Hinode/EIS. ApJ721:744–749, DOI
    10.1088/0004-637X/721/1/744, 1008.1823

Klimchuk JA (2006) On Solving the Coronal Heating Problem.
    Sol. Phys.234(1):41–77, DOI 10.1007/s11207-006-0055-z, astro-ph/0511841

Kolotkov DY, Nakariakov VM, Zavershinskii DI (2019) Damping of slow mag-
    netoacoustic oscillations by the misbalance between heating and cooling pro-
    cesses in the solar corona. A&A628:A133, DOI 10.1051/0004-6361/201936072,
    1907.07051

Kolotkov DY, Duckenfield TJ, Nakariakov VM (2020) Seismological constraints on
    the solar coronal heating function. arXiv e-prints arXiv:2010.03364, 2010.03364

Krishna Prasad S, Raes JO, Van Doorsselaere T, Magyar N, Jess DB (2018) The
    Polytropic Index of Solar Coronal Plasma in Sunspot Fan Loops and Its Temper-
    ature Dependence. ApJ868(2):149, DOI 10.3847/1538-4357/aae9f5, 1810.08449

Kudoh T, Shibata K (1999) Alfvén Wave Model of Spicules and Coronal Heating.
    ApJ514:493–505, DOI 10.1086/306930

Kumar P, Manoharan PK (2013) Eruption of a plasma blob, associated M-class
    flare, and large-scale extreme-ultraviolet wave observed by SDO. A&A553:A109,
    DOI 10.1051/0004-6361/201220283, 1304.0165

Kuperus M, Ionson JA, Spicer DS (1981) On the theory of coronal heating mech-
    anisms. ARA&A19:7–40, DOI 10.1146/annurev.aa.19.090181.000255

Lau YT, Siregar E (1996) Nonlinear Alfven Wave Propagation in the Solar Wind.
    ApJ465:451, DOI 10.1086/177432

Lemen JR, Title AM, Akin DJ, Boerner PF, Chou C, Drake JF, Duncan DW,
    Edwards CG, Friedlaender FM, Heyman GF, Hurlburt NE, Katz NL, Kushner
    GD, Levay M, Lindgren RW, Mathur DP, McFeaters EL, Mitchell S, Rehse
    RA, Schrijver CJ, Springer LA, Stern RA, Tarbell TD, Wuelser JP, Wolfson
    CJ, Yanari C, Bookbinder JA, Cheimets PN, Caldwell D, Deluca EE, Gates R,
    Golub L, Park S, Podgorski WA, Bush RI, Scherrer PH, Gummin MA, Smith
    P, Auker G, Jerram P, Pool P, Soufli R, Windt DL, Beardsley S, Clapp M,

Lang J, Waltham N (2012) The Atmospheric Imaging Assembly (AIA) on the Solar Dynamics Observatory (SDO). Sol. Phys.275(1-2):17–40, DOI 10.1007/s11207-011-9776-8

Leroy B (1980) Propagation of waves in an atmosphere in the presence of a magnetic field. II - The reflection of Alfven waves. A&A91(1-2):136–146

Liu W, Ofman L (2014) Advances in Observing Various Coronal EUV Waves in the SDO Era and Their Seismological Applications (Invited Review). Sol. Phys.289:3233–3277, DOI 10.1007/s11207-014-0528-4, 1404.0670

Liu W, Nitta NV, Schrijver CJ, Title AM, Tarbell TD (2010) First SDO AIA Observations of a Global Coronal EUV "Wave": Multiple Components and "Ripples". ApJ723:L53–L59, DOI 10.1088/2041-8205/723/1/L53, 1201.0815

Liu W, Title AM, Zhao J, Ofman L, Schrijver CJ, Aschwanden MJ, De Pontieu B, Tarbell TD (2011) Direct Imaging of Quasi-periodic Fast Propagating Waves of ˜2000 km s$^{-1}$ in the Low Solar Corona by the Solar Dynamics Observatory Atmospheric Imaging Assembly. ApJ736:L13, DOI 10.1088/2041-8205/736/1/L13, 1106.3150

Liu W, Ofman L, Nitta NV, Aschwanden MJ, Schrijver CJ, Title AM, Tarbell TD (2012) Quasi-periodic Fast-mode Wave Trains within a Global EUV Wave and Sequential Transverse Oscillations Detected by SDO/AIA. ApJ753:52, DOI 10.1088/0004-637X/753/1/52, 1204.5470

Liu W, Ofman L, Broder B, Karlický M, Downs C (2016) Quasi-periodic fast-mode magnetosonic wave trains within coronal waveguides associated with flares and CMEs. In: American Institute of Physics Conference Series, vol 1720, p 040010, DOI 10.1063/1.4943821, 1512.07930

Magyar N, Van Doorsselaere T (2016) The Instability and Non-existence of Multistranded Loops When Driven by Transverse Waves. ApJ823:82, DOI 10.3847/0004-637X/823/2/82, 1604.04078

Magyar N, Van Doorsselaere T (2018) Assessing the Capabilities of Dynamic Coronal Seismology of Alfvénic Waves through Forward Modeling. ApJ856:144, DOI 10.3847/1538-4357/aab42c, 1804.02175

Magyar N, Van Doorsselaere T, Marcu A (2015) Numerical simulations of transverse oscillations in radiatively cooling coronal loops. A&A582:A117, DOI 10.1051/0004-6361/201526287, 1510.08760

Magyar N, Van Doorsselaere T, Gossens M (2017) Generalized phase mixing: Turbulence-like behaviour from unidirectionally propagating MHD waves. Scientific Reports 7:14820, DOI 10.1038/s41598-017-13660-1

Magyar N, Van Doorsselaere T, Goossens M (2019) Understanding Uniturbulence: Self-cascade of MHD Waves in the Presence of Inhomogeneities. ApJ882(1):50, DOI 10.3847/1538-4357/ab357c, 1907.10408

Matsumoto T (2016) Competition between shock and turbulent heating in coronal loop system. MNRAS463(1):502–511, DOI 10.1093/mnras/stw2032, 1606.06019

Matsumoto T (2018) Thermal responses in a coronal loop maintained by wave heating mechanisms. MNRAS476(3):3328–3335, DOI 10.1093/mnras/sty490, 1712.07377

Matsumoto T, Shibata K (2010) Nonlinear Propagation of Alfvén Waves Driven by Observed Photospheric Motions: Application to the Coronal Heating and Spicule Formation. ApJ710(2):1857–1867, DOI 10.1088/0004-637X/710/2/1857, 1001.4307

Matsumoto T, Suzuki TK (2014) Connecting the Sun and the solar wind: the self-consistent transition of heating mechanisms. MNRAS440(2):971–986, DOI 10.1093/mnras/stu310, 1402.0316

McIntosh SW, De Pontieu B (2012) Estimating the "Dark" Energy Content of the Solar Corona. ApJ761:138, DOI 10.1088/0004-637X/761/2/138, 1211.4178

McIntosh SW, de Pontieu B, Carlsson M, Hansteen V, Boerner P, Goossens M (2011) Alfvénic waves with sufficient energy to power the quiet solar corona and fast solar wind. Nature475:477–480, DOI 10.1038/nature10235

McLaughlin JA, Hood AW (2004) MHD wave propagation in the neighbourhood of a two-dimensional null point. A&A420:1129–1140, DOI 10.1051/0004-6361:20035900, 0712.1792

McLaughlin JA, Hood AW (2006) Magnetohydrodynamics wave propagation in the neighbourhood of two dipoles. A&A452(2):603–613, DOI 10.1051/0004-6361:20054575, 0712.1784

McLaughlin JA, Ofman L (2008) Three-dimensional Magnetohydrodynamic Wave Behavior in Active Regions: Individual Loop Density Structure. ApJ682(2):1338–1350, DOI 10.1086/588799

McLaughlin JA, De Moortel I, Hood AW, Brady CS (2009) Nonlinear fast magnetoacoustic wave propagation in the neighbourhood of a 2D magnetic X-point: oscillatory reconnection. A&A493(1):227–240, DOI 10.1051/0004-6361:200810465, 0901.1781

McLaughlin JA, de Moortel I, Hood AW (2011) Phase mixing of nonlinear visco-resistive Alfvén waves. A&A527:A149, DOI 10.1051/0004-6361/201015552, 1101.5945

Montes-Solís M, Arregui I (2020) Quantifying the evidence for resonant damping of coronal waves with foot-point wave power asymmetry. A&A640:L17, DOI 10.1051/0004-6361/201937237, 2008.03004

Moriyasu S, Kudoh T, Yokoyama T, Shibata K (2004) The nonlinear Alfvén wave model for solar coronal heating and nanoflares. ApJ601:L107 – L110

Morton RJ, Verth G, Jess DB, Kuridze D, Ruderman MS, Mathioudakis M, Erdélyi R (2012) Observations of ubiquitous compressive waves in the Sun's chromosphere. Nature Communications 3:1315, DOI 10.1038/ncomms2324, 1306.4124

Morton RJ, Tomczyk S, Pinto R (2015) Investigating Alfvénic wave propagation in coronal open-field regions. Nature Communications 6:7813, DOI 10.1038/ncomms8813

Morton RJ, Tomczyk S, Pinto RF (2016) A Global View of Velocity Fluctuations in the Corona below 1.3 R $_0$ with CoMP. ApJ828:89, DOI 10.3847/0004-637X/828/2/89, 1608.01831

Morton RJ, Weberg MJ, McLaughlin JA (2019) A basal contribution from p-modes to the Alfvénic wave flux in the Sun's corona. Nature Astronomy DOI 10.1038/s41550-018-0668-9, 1902.03811

Murawski K, Musielak ZE (2010) Linear Alfvén waves in the solar atmosphere. A&A518:A37, DOI 10.1051/0004-6361/201014394

Nakariakov VM, Ofman L, DeLuca EE, Roberts B, Davila JM (1999) TRACE observations of damped coronal loop oscillations: implications for coronal heating. Sci 285:862–864

Nakariakov VM, Ofman L, Arber TD (2000) Nonlinear dissipative spherical Alfvén waves in solar coronal holes. A&A353:741–748

Nakariakov VM, Pilipenko V, Heilig B, Jelínek P, Karlický M, Klimushkin DY, Kolotkov DY, Lee DH, Nisticò G, Van Doorsselaere T, Verth G, Zimovets IV (2016) Magnetohydrodynamic Oscillations in the Solar Corona and Earth's Magnetosphere: Towards Consolidated Understanding. Space Sci. Rev.200:75–203, DOI 10.1007/s11214-015-0233-0

Nakariakov VM, Afanasyev AN, Kumar S, Moon YJ (2017) Effect of Local Thermal Equilibrium Misbalance on Long-wavelength Slow Magnetoacoustic Waves. ApJ849(1):62, DOI 10.3847/1538-4357/aa8ea3

Nakariakov VM, Kosak MK, Kolotkov DY, Anfinogentov SA, Kumar P, Moon YJ (2019) Properties of Slow Magnetoacoustic Oscillations of Solar Coronal Loops by Multi-instrumental Observations. ApJ874(1):L1, DOI 10.3847/2041-8213/ab0c9f

Nakariakov VM, Anfinogentov SA, Antolin P, Jain R, Kolotkov DY, Kupriyanova EG, Li D, Magyar N, Nisticò G, Pascoe DJ, Srivastava AK, Terradas J, Vasheghani Farahani S, Verth G, Yuan D (2021) Kink oscillations of coronal loops. Space Science Reviews DOI submitted

Nechaeva A, Zimovets IV, Nakariakov VM, Goddard CR (2019) Catalog of Decaying Kink Oscillations of Coronal Loops in the 24th Solar Cycle. ApJS241:31, DOI 10.3847/1538-4365/ab0e86

Ning Z, Cao W, Okamoto TJ, Ichimoto K, Qu ZQ (2009) Small-scale oscillations in a quiescent prominence observed by HINODE/SOT. Prominence oscillations. A&A499:595–600, DOI 10.1051/0004-6361/200810853

Nisticò G, Nakariakov VM, Verwichte E (2013) Decaying and decayless transverse oscillations of a coronal loop. A&A552:A57, DOI 10.1051/0004-6361/201220676

Nisticò G, Pascoe DJ, Nakariakov VM (2014) Observation of a high-quality quasi-periodic rapidly propagating wave train using SDO/AIA. A&A569:A12, DOI 10.1051/0004-6361/201423763

Nykyri K, Otto A (2004) Influence of the Hall term on KH instability and reconnection inside KH vortices. Annales Geophysicae 22:935–949, DOI 10.5194/angeo-22-935-2004

Ofman L (2005) MHD Waves and Heating in Coronal Holes. Space Sci. Rev.120(1-2):67–94, DOI 10.1007/s11214-005-5098-1

Ofman L (2010) Wave Modeling of the Solar Wind. Living Reviews in Solar Physics 7(1):4, DOI 10.12942/lrsp-2010-4

Ofman L, Davila JM (1995) Alfvén wave heating of coronal holes and the relation to the high-speed solar wind. J. Geophys. Res.100(A12):23413–23426, DOI 10.1029/95JA02222

Ofman L, Davila JM (1998) Solar wind acceleration by large-amplitude nonlinear waves: Parametric study. J. Geophys. Res.103(A10):23677–23690, DOI 10.1029/98JA01996

Ofman L, Liu W (2018) Quasi-periodic Counter-propagating Fast Magnetosonic Wave Trains from Neighboring Flares: SDO/AIA Observations and 3D MHD Modeling. ApJ860(1):54, DOI 10.3847/1538-4357/aac2e8, 1805.00365

Ofman L, Davila JM, Steinolfson RS (1994) Nonlinear studies of coronal heating by the resonant absorption of Alfven waves. Geophys. Res. Lett.21:2259–+

Ofman L, Klimchuk JA, Davila JM (1998) A Self-consistent Model for the Resonant Heating of Coronal Loops: The Effects of Coupling with the Chromosphere. ApJ493:474, DOI 10.1086/305109

Ofman L, Nakariakov VM, DeForest CE (1999) Slow Magnetosonic Waves in Coronal Plumes. ApJ514(1):441–447, DOI 10.1086/306944

Ofman L, Liu W, Title A, Aschwanden M (2011) Modeling Super-fast Magnetosonic Waves Observed by SDO in Active Region Funnels. ApJ740:L33, DOI 10.1088/2041-8205/740/2/L33

Okamoto TJ, De Pontieu B (2011) Propagating Waves Along Spicules. ApJ736(2):L24, DOI 10.1088/2041-8205/736/2/L24, 1106.4270

Okamoto TJ, Antolin P, De Pontieu B, Uitenbroek H, Van Doorsselaere T, Yokoyama T (2015) Resonant Absorption of Transverse Oscillations and Associated Heating in a Solar Prominence. I. Observational Aspects. ApJ809:71, DOI 10.1088/0004-637X/809/1/71, 1506.08965

Oran R, Landi E, van der Holst B, Sokolov IV, Gombosi TI (2017) Alfvén Wave Turbulence as a Coronal Heating Mechanism: Simultaneously Predicting the Heating Rate and the Wave-induced Emission Line Broadening. ApJ845(2):98, DOI 10.3847/1538-4357/aa7fec

Pagano P, De Moortel I (2017) Contribution of mode-coupling and phase-mixing of Alfvén waves to coronal heating. A&A601:A107, DOI 10.1051/0004-6361/201630059

Pagano P, De Moortel I (2019) Contribution of observed multi frequency spectrum of Alfvén waves to coronal heating. A&A623:A37, DOI 10.1051/0004-6361/201834158, 1901.02310

Pagano P, Pascoe DJ, De Moortel I (2018) Contribution of phase-mixing of Alfvén waves to coronal heating in multi-harmonic loop oscillations. A&A616:A125, DOI 10.1051/0004-6361/201732251, 1804.10562

Pagano P, Van Damme HJ, Antolin P, De Moortel I (2019) MHD simulations of the in situ generation of kink and sausage waves in the solar corona by collision of dense plasma clumps. A&A626:A53, DOI 10.1051/0004-6361/201935539, 1905.03749

Pant V, Magyar N, Van Doorsselaere T, Morton RJ (2019) Investigating "Dark" Energy in the Solar Corona Using Forward Modeling of MHD Waves. ApJ881(2):95, DOI 10.3847/1538-4357/ab2da3, 1906.10941

Parker EN (1986) Equilibrium of magnetic fields with arbitrary interweaving of the lines of force. II. Discontinuities in the field. Geophysical and Astrophysical Fluid Dynamics 35(4):277–301, DOI 10.1080/03091928608245896

Parker EN (1991) The phase mixing of Alfven waves, coordinated modes, and coronal heating. ApJ376:355–363, DOI 10.1086/170285

Parnell CE, De Moortel I (2012) A contemporary view of coronal heating. Royal Society of London Philosophical Transactions Series A 370:3217–3240, DOI 10.1098/rsta.2012.0113, 1206.6097

Pascoe DJ, De Moortel I (2014) Standing Kink Modes in Three-dimensional Coronal Loops. ApJ784:101, DOI 10.1088/0004-637X/784/2/101

Pascoe DJ, de Moortel I, McLaughlin JA (2009) Impulsively generated oscillations in a 3D coronal loop. A&A505:319–327, DOI 10.1051/0004-6361/200912270

Pascoe DJ, Wright AN, De Moortel I (2010) Coupled Alfvén and Kink Oscillations in Coronal Loops. ApJ711:990–996, DOI 10.1088/0004-637X/711/2/990

Pascoe DJ, Wright AN, De Moortel I (2011) Propagating Coupled Alfvén and Kink Oscillations in an Arbitrary Inhomogeneous Corona. ApJ731:73, DOI 10.1088/0004-637X/731/1/73

Pascoe DJ, Russell AJB, Anfinogentov SA, Simões PJA, Goddard CR, Nakariakov VM, Fletcher L (2017) Seismology of contracting and expanding coronal loops using damping of kink oscillations by mode coupling. A&A607:A8, DOI 10.1051/0004-6361/201730915

Pascoe DJ, Smyrli A, Van Doorsselaere T (2020) Tracking and Seismological Analysis of Multiple Coronal Loops in an Active Region. ApJ898(2):126, DOI 10.3847/1538-4357/aba0a6

Perez JC, Chandran BDG (2013) Direct Numerical Simulations of Reflection-driven, Reduced Magnetohydrodynamic Turbulence from the Sun to the Alfvén Critical Point. ApJ776:124, DOI 10.1088/0004-637X/776/2/124

Piddington JH (1956) Solar atmospheric heating by hydromagnetic waves. MNRAS116:314, DOI 10.1093/mnras/116.3.314

Poedts S, Goossens M, Kerner W (1990) On the Efficiency of Coronal Loop Heating by Resonant Absorption. ApJ360:279, DOI 10.1086/169118

Qu ZN, Jiang LQ, Chen SL (2017) Observations of a Fast-mode Magnetosonic Wave Propagating along a Curving Coronal Loop on 2011 November 11. ApJ851:41, DOI 10.3847/1538-4357/aa9beb

Reale F (2014) Coronal Loops: Observations and Modeling of Confined Plasma. Living Reviews in Solar Physics 11(1):4, DOI 10.12942/lrsp-2014-4

Reep JW, Bradshaw SJ, Klimchuk JA (2013) Diagnosing the Time Dependence of Active Region Core Heating from the Emission Measure. II. Nanoflare Trains. ApJ764(2):193, DOI 10.1088/0004-637X/764/2/193, 1303.4466

Rempel M (2017) Extension of the MURaM Radiative MHD Code for Coronal Simulations. ApJ834(1):10, DOI 10.3847/1538-4357/834/1/10, 1609.09818

Rial S, Arregui I, Terradas J, Oliver R, Ballester JL (2010) Three-dimensional Propagation of Magnetohydrodynamic Waves in Solar Coronal Arcades. ApJ713(1):651–661, DOI 10.1088/0004-637X/713/1/651, 1002.0469

Rosner R, Tucker WH, Vaiana GS (1978) Dynamics of the quiescent solar corona. ApJ220:643–645, DOI 10.1086/155949

Ruderman MS, Berghmans D, Goossens M, Poedts S (1997a) Direct excitation of resonant torsional Alfven waves by footpoint motions. A&A320:305–318

Ruderman MS, Goossens M, Ballester JL, Oliver R (1997b) Resonant Alfven waves in coronal arcades driven by footpoint motions. A&A328:361–370

Russell AJB, Simões PJA, Fletcher L (2015) A unified view of coronal loop contraction and oscillation in flares. A&A581:A8, DOI 10.1051/0004-6361/201525746, 1506.07716

Sabri S, Vasheghani Farahani S, Ebadi H, Hosseinpour M, Fazel Z (2018) Alfvén wave dynamics at the neighbourhood of a 2.5D magnetic null-point. MNRAS479(4):4991–4997, DOI 10.1093/mnras/sty1407

Schrijver CJ, Title AM, Berger TE, Fletcher L, Hurlburt NE, Nightingale RW, Shine RA, Tarbell TD, Wolfson J, Golub L, Bookbinder JA, Deluca EE, McMullen RA, Warren HP, Kankelborg CC, Handy BN, de Pontieu B (1999) A new view of the solar outer atmosphere by the Transition Region and Coronal Explorer. Sol. Phys.187:261–302

Sekse DH, Rouppe van der Voort L, De Pontieu B, Scullion E (2013) Interplay of Three Kinds of Motion in the Disk Counterpart of Type II Spicules: Upflow, Transversal, and Torsional Motions. ApJ769:44, DOI 10.1088/0004-637X/769/1/44, 1304.2304

Selwa M, Ofman L (2009) 3-D numerical simulations of coronal loops oscillations. Annales Geophysicae 27(10):3899–3908, DOI 10.5194/angeo-27-3899-2009

Shen Y, Liu Y, Song T, Tian Z (2018) A Quasi-periodic Fast-propagating Magnetosonic Wave Associated with the Eruption of a Magnetic Flux Rope. ApJ853:1, DOI 10.3847/1538-4357/aaa3ff, 1712.09045

Shen YD, Liu Y (2012) Observational Study of the Quasi-periodic Fast-propagating Magnetosonic Waves and the Associated Flare on 2011 May 30. ApJ753:53, DOI 10.1088/0004-637X/753/1/53, 1204.6649

Shen YD, Liu Y, Su JT, Li H, Zhang XF, Tian ZJ, Zhao RJ, Elmhamdi A (2013) Observations of a Quasi-periodic, Fast-Propagating Magnetosonic Wave in Multiple Wavelengths and Its Interaction with Other Magnetic Structures. Sol. Phys.288:585–602, DOI 10.1007/s11207-013-0395-4, 1307.6099

Shen YD, Liu Y, Song T, Tian Z (2017) A quasi-periodic fast-propagating magnetosonic wave associated with the eruption of a magnetic flux rope. ArXiv e-prints 1712.09045

Shoda M, Suzuki TK, Asgari-Targhi M, Yokoyama T (2019) Three-dimensional Simulation of the Fast Solar Wind Driven by Compressible Magnetohydrodynamic Turbulence. ApJ880(1):L2, DOI 10.3847/2041-8213/ab2b45, 1905.11685

Singh J, Sakurai T, Ichimoto K, Muneer S, Raveendran AV (2006) Spectroscopic Studies of Solar Corona VIII. Temperature and Non-Thermal Variations in Steady Coronal Structures. Sol. Phys.236:245–262, DOI 10.1007/s11207-006-0104-7

Soler R, Terradas J (2015) Magnetohydrodynamic Kink Waves in Nonuniform Solar Flux Tubes: Phase Mixing and Energy Cascade to Small Scales. ApJ803(1):43, DOI 10.1088/0004-637X/803/1/43, 1502.03949

Soler R, Terradas J, Oliver R, Ballester JL (2017) Propagation of Torsional Alfvén Waves from the Photosphere to the Corona: Reflection, Transmission, and Heating in Expanding Flux Tubes. ApJ840(1):20, DOI 10.3847/1538-4357/aa6d7f

Soler R, Terradas J, Oliver R, Ballester JL (2019) Energy Transport and Heating by Torsional Alfvén Waves Propagating from the Photosphere to the Corona in the Quiet Sun. ApJ871(1):3, DOI 10.3847/1538-4357/aaf64c, 1812.01323

Spicer DS (1977) An unstable arch model of a solar flare. Sol. Phys.53(2):305–345, DOI 10.1007/BF00160276

Srivastava AK, Shetye J, Murawski K, Doyle JG, Stangalini M, Scullion E, Ray T, Wójcik DP, Dwivedi BN (2017) High-frequency torsional Alfvén waves as an energy source for coronal heating. Scientific Reports 7:43147, DOI 10.1038/srep43147

Srivastava AK, Mishra SK, Jelínek P, Samanta T, Tian H, Pant V, Kayshap P, Banerjee D, Doyle JG, Dwivedi BN (2019) On the Observations of Rapid Forced Reconnection in the Solar Corona. ApJ887(2):137, DOI 10.3847/1538-4357/ab4a0c, 1901.07971

Stangalini M, Jafarzadeh S, Ermolli I, Erdélyi R, Jess DB, Keys PH, Giorgi F, Murabito M, Berrilli F, Del Moro D (2018) Propagating Spectropolarimetric Disturbances in a Large Sunspot. ApJ869(2):110, DOI 10.3847/1538-4357/aaec7b, 1810.12595

Stepanov AV, Zaitsev VV, Nakariakov VM (2012) Coronal Seismology: Waves and Oscillations in Stellar Coronae Flare Plasma. DOI 10.1002/9783527645985

Suzuki TK (2008) Coronal heating and wind acceleration by nonlinear Alfvén waves ? global simulations with gravity, radiation, and conduction. Nonlinear

Processes in Geophysics 15(2):295–304, URL `https://hal.archives-ouvertes.fr/hal-00302984`

Suzuki TK (2012) Solar wind and its evolution. Earth, Planets, and Space 64(2):201–206, DOI 10.5047/eps.2011.04.012, `1104.3660`

Suzuki TK, Inutsuka S (2005) Making the Corona and the Fast Solar Wind: A Self-consistent Simulation for the Low-Frequency Alfvén Waves from the Photosphere to 0.3 AU. ApJ632:L49–L52, DOI 10.1086/497536, `arXiv:astro-ph/0506639`

Suzuki TK, Inutsuka SI (2006) Solar winds driven by nonlinear low-frequency Alfvén waves from the photosphere: Parametric study for fast/slow winds and disappearance of solar winds. Journal of Geophysical Research (Space Physics) 111(A6):A06101, DOI 10.1029/2005JA011502, `astro-ph/0511006`

Terradas J, Arregui I (2018) Temporal and Spatial Scales for Coronal Heating by Alfvén Wave Dissipation in Transverse Loop Oscillations. Research Notes of the American Astronomical Society 2(4):196, DOI 10.3847/2515-5172/aaeb26

Terradas J, Andries J, Goossens M (2007) Coronal loop oscillations: energy considerations and initial value problem. A&A469:1135–1143, DOI 10.1051/0004-6361:20077404

Terradas J, Andries J, Goossens M, Arregui I, Oliver R, Ballester JL (2008a) Nonlinear Instability of Kink Oscillations due to Shear Motions. ApJ687:L115–L118, DOI 10.1086/593203, `0809.3664`

Terradas J, Arregui I, Oliver R, Ballester JL, Andries J, Goossens M (2008b) Resonant Absorption in Complicated Plasma Configurations: Applications to Multistranded Coronal Loop Oscillations. ApJ679:1611–1620, DOI 10.1086/586733, `arXiv:0802.0591`

Terradas J, Magyar N, Van Doorsselaere T (2018) Effect of Magnetic Twist on Nonlinear Transverse Kink Oscillations of Line-tied Magnetic Flux Tubes. ApJ853:35, DOI 10.3847/1538-4357/aa9d0f

Thurgood JO, McLaughlin JA (2013) Nonlinear Alfvén wave dynamics at a 2D magnetic null point: ponderomotive force. A&A555:A86, DOI 10.1051/0004-6361/201321338, `1305.7073`

Tian H, McIntosh SW, Wang T, Ofman L, De Pontieu B, Innes DE, Peter H (2012) Persistent Doppler Shift Oscillations Observed with Hinode/EIS in the Solar Corona: Spectroscopic Signatures of Alfvénic Waves and Recurring Upflows. ApJ759:144, DOI 10.1088/0004-637X/759/2/144, `1209.5286`

Tian H, DeLuca EE, Cranmer SR, De Pontieu B, Peter H, Martínez-Sykora J, Golub L, McKillop S, Reeves KK, Miralles MP, McCauley P, Saar S, Testa P, Weber M, Murphy N, Lemen J, Title A, Boerner P, Hurlburt N, Tarbell TD, Wuelser JP, Kleint L, Kankelborg C, Jaeggli S, Carlsson M, Hansteen V, McIntosh SW (2014) Prevalence of small-scale jets from the networks of the solar transition region and chromosphere. Science 346(6207):1255711, DOI 10.1126/science.1255711, `1410.6143`

Tomczyk S, McIntosh SW (2009) Time-Distance Seismology of the Solar Corona with CoMP. ApJ697:1384–1391, DOI 10.1088/0004-637X/697/2/1384, `0903.2002`

Tomczyk S, McIntosh SW, Keil SL, Judge PG, Schad T, Seeley DH, Edmondson J (2007) Alfven Waves in the Solar Corona. Science 317(5842):1192–1196, DOI 10.1126/science.1143304, URL `http://www.sciencemag.org/cgi/content/abstract/317/5842/1192`, `http://www.sciencemag.org/cgi/reprint/317/5842/`

`1192.pdf`

Tomczyk S, Card GL, Darnell T, Elmore DF, Lull R, Nelson PG, Streander KV, Burkepile J, Casini R, Judge PG (2008) An Instrument to Measure Coronal Emission Line Polarization. Sol. Phys.247(2):411–428, DOI 10.1007/s11207-007-9103-6

Tu CY, Zhou C, Marsch E, Xia LD, Zhao L, Wang JX, Wilhelm K (2005) Solar Wind Origin in Coronal Funnels. Science 308(5721):519–523, DOI 10.1126/science.1109447

Uchida Y, Kaburaki O (1974) Excess Heating of Corona and Chromosphere Above Magnetic Regions by Non-Linear Alfvén Waves. Sol. Phys.35:451–466, DOI 10.1007/BF00151968

Usmanov AV, Matthaeus WH, Goldstein ML, Chhiber R (2018) The Steady Global Corona and Solar Wind: A Three-dimensional MHD Simulation with Turbulence Transport and Heating. ApJ865(1):25, DOI 10.3847/1538-4357/aad687

van Ballegooijen AA, Asgari-Targhi M (2018) The Heating of Coronal Loops in Solar Active Regions. In: Journal of Physics Conference Series, Journal of Physics Conference Series, vol 1100, p 012027, DOI 10.1088/1742-6596/1100/1/012027

van Ballegooijen AA, Asgari-Targhi M, Cranmer SR, DeLuca EE (2011) Heating of the Solar Chromosphere and Corona by Alfvén Wave Turbulence. ApJ736:3, DOI 10.1088/0004-637X/736/1/3, `1105.0402`

van Ballegooijen AA, Asgari-Targhi M, Voss A (2017) The Heating of Solar Coronal Loops by Alfvén Wave Turbulence. ApJ849:46, DOI 10.3847/1538-4357/aa9118, `1710.05074`

Van Damme HJ, De Moortel I, Pagano P, Johnston CD (2020) Chromospheric evaporation and phase mixing of Alfvén waves in coronal loops. A&A635:A174, DOI 10.1051/0004-6361/201937266

van der Holst B, Sokolov IV, Meng X, Jin M, Manchester WB IV, Tóth G, Gombosi TI (2014) Alfvén Wave Solar Model (AWSoM): Coronal Heating. ApJ782:81, DOI 10.1088/0004-637X/782/2/81, `1311.4093`

Van Doorsselaere T, Nakariakov VM, Verwichte E (2008) Detection of waves in the solar corona: kink or Alfvén? ApJ676:L73–L75

Van Doorsselaere T, Gijsen SE, Andries J, Verth G (2014) Energy Propagation by Transverse Waves in Multiple Flux Tube Systems Using Filling Factors. ApJ795:18, DOI 10.1088/0004-637X/795/1/18

Vasheghani Farahani S, Hejazi SM (2017) Coronal Jet Collimation by Nonlinear Induced Flows. ApJ844(2):148, DOI 10.3847/1538-4357/aa7da5

Vasheghani Farahani S, Nakariakov VM, Van Doorsselaere T (2010) Long-wavelength torsional modes of solar coronal plasma structures. A&A517:A29+, DOI 10.1051/0004-6361/201014502

Vasheghani Farahani S, Nakariakov VM, van Doorsselaere T, Verwichte E (2011) Nonlinear long-wavelength torsional Alfvén waves. A&A526:A80+, DOI 10.1051/0004-6361/201016063

Vasheghani Farahani S, Nakariakov VM, Verwichte E, Van Doorsselaere T (2012) Nonlinear evolution of torsional Alfvén waves. A&A544:A127, DOI 10.1051/0004-6361/201219569

Verth G, Terradas J, Goossens M (2010) Observational Evidence of Resonantly Damped Propagating Kink Waves in the Solar Corona. ApJ718(2):L102–L105, DOI 10.1088/2041-8205/718/2/L102, `1007.1080`

Walsh RW, Ireland J (2003) The heating of the solar corona. A&A Rev.12(1):1–41, DOI 10.1007/s00159-003-0021-9

Wang T (2011) Standing Slow-Mode Waves in Hot Coronal Loops: Observations, Modeling, and Coronal Seismology. Space Sci. Rev.158:397–419, DOI 10.1007/s11214-010-9716-1, 1011.2483

Wang T, Ofman L, Davila JM, Su Y (2012) Growing Transverse Oscillations of a Multistranded Loop Observed by SDO/AIA. ApJ751(2):L27, DOI 10.1088/2041-8205/751/2/L27, 1204.1376

Wang TJ (2016) Waves in Solar Coronal Loops. Washington DC American Geophysical Union Geophysical Monograph Series 216:395–418, DOI 10.1002/9781119055006.ch23, 1803.11329

Wang TJ, Ofman L, Yuan D, Reale F, Kolotkov DY, Srivastava AK (2021) Slow-Mode Magnetoacoustic Waves in Coronal Loops. Space Science Reviews DOI submitted

Warnecke J, Chen F, Bingert S, Peter H (2017) Current systems of coronal loops in 3D MHD simulations. A&A607:A53, DOI 10.1051/0004-6361/201630095, 1611.06170

Withbroe GL, Noyes RW (1977) Mass and energy flow in the solar chromosphere and corona. ARA&A15:363–387, DOI 10.1146/annurev.aa.15.090177.002051

Wójcik D, Murawski K, Musielak ZE, Konkol P, Mignone A (2017) Numerical Simulations of Torsional Alfvén Waves in Axisymmetric Solar Magnetic Flux Tubes. Sol. Phys.292(2):31, DOI 10.1007/s11207-017-1058-7, 1701.04594

Wójcik D, Kuźma B, Murawski K, Musielak ZE (2020) Wave heating of the solar atmosphere without shocks. A&A635:A28, DOI 10.1051/0004-6361/201936938

Woolsey LN, Cranmer SR (2015) Time-dependent Turbulent Heating of Open Flux Tubes in the Chromosphere, Corona, and Solar Wind. ApJ811(2):136, DOI 10.1088/0004-637X/811/2/136, 1509.00377

Yang Z, Bethge C, Tian H, Tomczyk S, Morton R, Del Zanna G, McIntosh SW, Karak BB, Gibson S, Samanta T, He J, Chen Y, Wang L (2020a) Global maps of the magnetic field in the solar corona. Science 369(6504):694–697, DOI 10.1126/science.abb4462, 2008.03136

Yang Z, Tian H, Tomczyk S, Morton R, Bai X, Samanta T, Chen Y (2020b) Mapping the magnetic field in the solar corona through magnetoseismology. Sci China Tech Sci 63(11):2357–2368, DOI 10.1007/s11431-020-1706-9, 2008.03146

Yuan D, Shen YD, Liu Y, Nakariakov VM, Tan B, Huang J (2013) Distinct propagating fast wave trains associated with flaring energy releases. A&A554:A144, DOI 10.1051/0004-6361/201321435

Zavershinskii DI, Kolotkov DY, Nakariakov VM, Molevich NE, Ryashchikov DS (2019) Formation of quasi-periodic slow magnetoacoustic wave trains by the heating/cooling misbalance. Physics of Plasmas 26(8):082113, DOI 10.1063/1.5115224, 1907.08168

Zhang Y, Zhang J, Wang J, Nakariakov VM (2015) Coexisting fast and slow propagating waves of the extreme-UV intensity in solar coronal plasma structures. A&A581:A78, DOI 10.1051/0004-6361/201525621

Zhugzhda YD (1996) Force-free thin flux tubes: Basic equations and stability. Physics of Plasmas 3:10–21, DOI 10.1063/1.871836

Zimovets IV, Nakariakov VM (2015) Excitation of kink oscillations of coronal loops: statistical study. A&A577:A4, DOI 10.1051/0004-6361/201424960